# DESIGN OF LIPID-BASED DELIVERY SYSTEMS FOR IMPROVING LYMPHATIC TRANSPORT AND BIOAVAILABILITY OF DELTA-TOCOPHEROL AND NOBILETIN

By

CHUNXIN XIA

A thesis submitted to the

Graduate School-New Brunswick

Rutgers, The State University of New Jersey

in partial fulfillment of the requirements

for the degree of

Master of Science

Graduate Program in Food Science

written under the direction of

Dr. Qingrong Huang

and approved by

_____

_____

_____

_____

New Brunswick, New Jersey

October 2015

**ABSTRACT OF THE THESIS**

**Design of Lipid-Based Delivery Systems for Improving Lymphatic Transport and Bioavailability of Delta-Tocopherol and Nobiletin**

**by Chunxin Xia**

**Thesis Directors:**

**Dr. Qingrong Huang**

Lymphatic drug transport can confer bioavailability advantage by avoiding the first-pass metabolism normally observed in the portal vein hepatic route. It was reported that long chain lipid-based delivery systems can stimulate the formation of chylomicron and thus promote the lymphatic transport of drugs. In this study, a novel delta-tocopherol (δ-T) loaded Solid Lipid Nanoparticle (SLN) system was developed to investigate its effect on promoting the lymphatic transport of δ-T. The δ-T SLN was prepared with hot melt emulsification method by using glyceryl behenate (compritol®888) as the lipid phase and lecithin (PC75) as the emulsifier. Formula configuration, processing condition and loading capacity were carefully optimized. Physicochemical properties (particle size, surface charge, morphology) were also characterized. Moreover, excellent stability of the developed δ-T SLN in the gastrointestinal environment was observed by using an *in vitro* digestion model. Further investigations of the SLN in stimulating δ-T lymphatic transport were performed on mice without cannulation. Compared with the control group (δ-T corn oil dispersion), much lower δ-T levels in both blood and liver indicated reduced portal vein and hepatic transport of δ-T in the form of SLN. On the other hand, significantly

higher concentrations of δ-T were observed in thymus, a major lymphatic tissue, indicating improved lymphatic transport of δ-T with the SLN delivery system. Finally, the far less excreted δ-T level in feces further confirmed improved lymphatic transport and overall bioavailability of δ-T by using SLN system.

Nobiletin (NOB), one of most abundant polymethoxyflavones (PMFs) found in *Citrus* genus, has a low solubility in both water and oil at ambient temperatures. Thus it tends to form crystals when the loading exceeds its saturation level in the carrier system. This character greatly impaired its bioavailability and application. To overcome these problems, an O/W nanoemulsion was developed for NOB delivery with the presence of cremophor EL (a polyethoxylated excipient). The developed formulation can achieve a high NOB loading (0.5 wt%) with significantly reduced crystallinity and excellent physical stability. NOB's bioaccessibility and permeation rate across the enterocytes were demonstrated to be significantly improved by the *in vitro* digestion model and Caco-2 cell monolayer, respectively. It is thus predictable that NOB's bioavailability can be improved with our developed nanoemulsion formulation.

## ACKNOWLEGEMENT

I am deeply indebted to my advisor, Dr. Qingrong Huang, for his guidance and encouragement through these three years, and for his confidence in me to complete my Master's degree. Besides the guidance in my research, Dr. Huang is also very supportive and helpful with my career development and gave me many insightful suggestions.

My appreciation is extended to my co-advisor Dr. Chung S. Yang. This thesis would not have been possible without the guidance and help from Dr. Yang, whose intelligence and vision inspired me on the Solid Lipid Nanoparticle project. At the same time, I would also like to acknowledge Dr. Chi-Tang Ho, for being my committee member, and for all his suggestions and encouragement.

I would like to thank all of my labmates and colleagues at Department of Food Science and Ernest Mario School of Pharmacy. I greatly appreciate the help from Marlon Lee and Anna Liu for the animal experiments. Thanks to Dr. Yuwen Ting for training me on many experimental skills. Special thanks to Huijuan Zheng and Muwen Lu, who are always supportive in my tough moments on research. I also appreciate my undergraduate assistant Nichole Dzeidzic, who worked with me during my second year. We enjoyed the time working together on the nanoemulsion project.

Last but not least, I would like to thank my parents, and my beloved, encouraging and thoughtful husband, Qin Zhao, for the unconditional love and support during my most difficult time.

## TABLE OF CONTENTS

## LIST OF TABLES

## LIST OF FIGURES

# CHAPTER 1: BACKGROUND INTRODUCTION

## 1.1. Lymphatic system & intestinal lymphatic system

Lymphatic system is a drainage network spread throughout the body. It exists nearly in all parts of the body including the central nervous system (*1*). And it consists of lymph and lymphatic pathways, such as lymphatic capillaries, vessels, ducts etc. Main organs of the lymphatic system include bone marrow, lymph nodes, thymus, and spleen **(Fig. 1)** (*2, 3*). The lymphatic system, as people generally know, plays an important role in helping body to defend the tissues against infection by filtering particles from the lymph and by supporting the activities of the lymphocytes. In addition, it transports various immune cells and other elements essential to the immune system (*4, 5*). While the major and well recognized function of the lymphatics is actually to drain the capillary bed and return extracellular fluid to the systemic circulation, thus maintaining the body's water balance, just as blood vessels do (*6*).

However, the structure and function of the lymphatics throughout the body are not uniform. Different types of lymphatics perform specialized roles in specific areas. Among which, the intestinal lymphatics (**Fig. 1**) that play an essential role in transportation of dietary fat and lipid soluble substances to the systemic circulation (*7*) have gained our special attention, since it is associated with a special delivery and absorption pathway of the ingested nutrients or drugs after going through the gastrointestinal (GI) tract. In most cases, majority of the orally administered nutrients or drugs gain access to the systemic circulation by absorption into the portal vein blood. However, for some extremely lipophilic compounds, transport via the intestinal lymphatics provides an additional route.

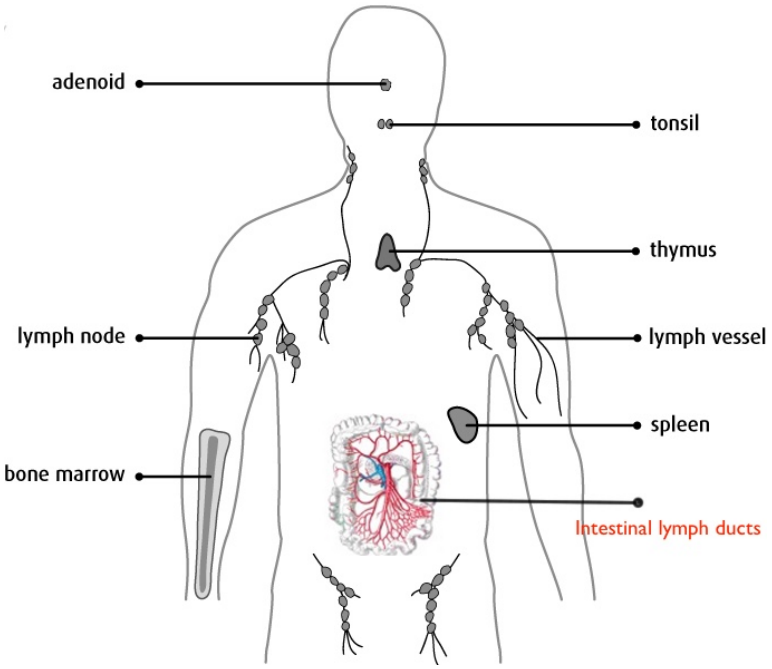


**Figure 1.** Lymphatic system and intestinal lymphatics (Modified from an online source: http://www.cancer.ca/en/cancer-information/cancer-type/hodgkin-lymphoma/anatomy-and-physiology)

Lymph drains via the lymphatic capillaries to the mesenteric lymph duct, and flows through to the cysterna chyli and from there into the thoracic duct. Eventually the lymph is reunited into the systemic circulation at the junction of the left jugular and the left subclavian veins (*8*). Thanks to this unique anatomy, nutraceuticals and drugs successfully transported via the intestinal lymphatics may confer bioavailability advantages by avoiding the hepatic first pass metabolism (*7*).

Nevertheless, exogenous compounds absorbed via the intestinal lymph are generally transported in association with the lipid core of intestinal lipoproteins. It is

widely accepted that co-administration of lipids, and the corresponding lipid digestion and absorption can stimulate and promote the lymphatic transport of lipophilic nutraceuticals and drugs (*9, 10*). Therefore, the mechanisms and importance of lipid digestion and absorption will also need to be addressed.

**1.2. Lipid digestion and absorption**

The detailed lipid digestion and absorption process have been extensively reviewed before (*11-15*). In principal, the big category of lipids or dietary fats is composed of different types of fatty acids, triglycerides, phospholipids, cholesterols, cholesteryl esters, and many other sterols (*16*). In this thesis, we mainly focus on triglycerides (the major form of dietary lipids) with different chain lengths, and fatty acids, mono-/di-glycerides involved in the triglycerides digestion and absorption.

Although the digestion of triglycerides is initiated in the oral cavity by lingual lipase and enhanced by the activity of gastric lipase in stomach, still more than 70% of the lipids that enters the upper duodenum are remain triglycerides (*13*). Therefore, most triglycerides digestion occurs in the small intestine with the action of pancreatic lipase and bile secreted from the gallbladder. Bile is composed of bile salts, phospholipid, and free cholesterol, which is an inherent emulsifier that helps to solubilize the intestinal contents (chyme) and maximizes the rate of lipid digestion. Pancreatic lipases only hydrolyze the fatty acids in the sn-1, and sn-3 positions of the triglycerides, with the sn-2 position resistant to the hydrolysis, resulting with a 2-monoglyceride and two free fatty acids (*17*). Then the hydrolytic products of triglyceride along with bile salts, phospholipids, and other fat-soluble substances form micelles in the small intestine lumen. Free fatty acids and cholesterol will also be incorporated into the micellar structure (*18*).

Absorption of micellar components into intestinal epithelial cells depends on the penetration of micelles across the unstirred water layer that separates the intestinal lumen from the brush border of the small intestine. The relatively small size (3-10 nm) and hydrophilic nature of the micelles facilitate this diffusion process. After the lipid digestion products (fatty acids, monoglycerides) enter into the enterocytes, their absorption routes are mainly dependent on the chain length of the lipids.

The traditional view is that the fatty acids with chain length greater than 12-C will migrate from the absorptive site to the endoplasmic reticulum and re-esterify into triglycerides. It will then be packed into the chylomicron, a major transport lipoprotein. Chylomicrons are secreted into the mesenteric lymph from where they drain via the thoracic lymph duct into the systemic circulation. In contrast, for the short / middle chain lipids (usually with ≤ 10-C), different absorption route occurs. They are absorbed directly into the portal vein blood for the systemic circulation (*19*). The simplified lipid digestion and absorption process can be summarized in the following figures **(Fig. 2, 3)**. It is necessary to mention that in practical, the chain-length dependent route of the lipid transport is not absolute. The above mentioned trend is primarily observed; while still few reports indicated some rare cases that lymphatic transport of medium chain fatty acids or portal blood absorption of long chain fatty acids (*20-22*). Thus it is an interesting research area need to be further explored with more diverse lipid based systems.

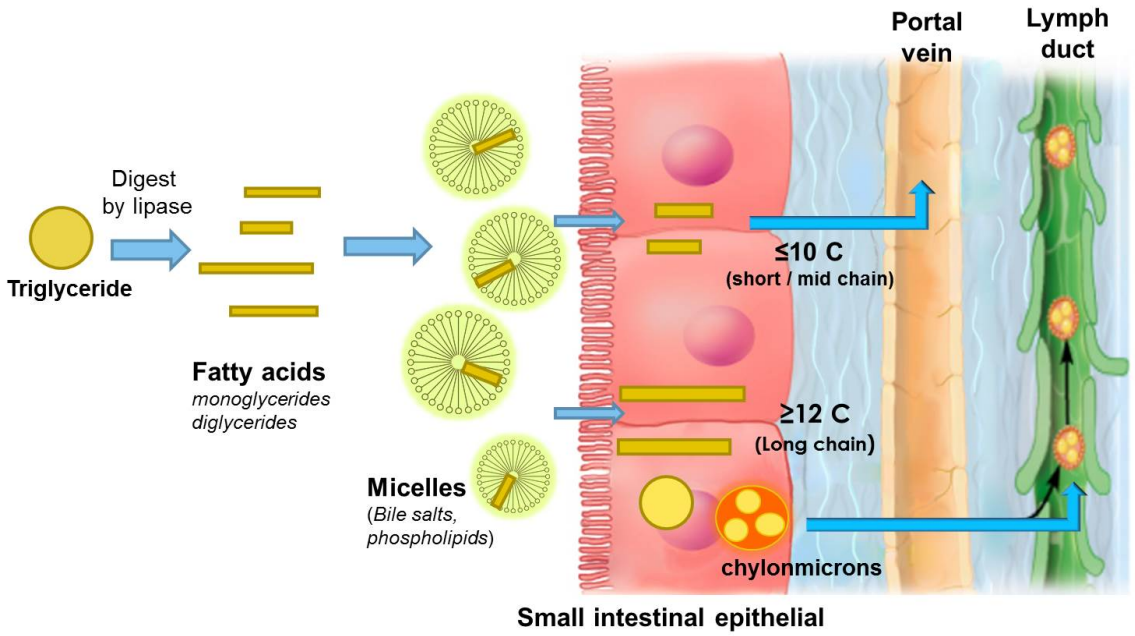


**Figure 2.** The simplified digestion and absorption process of lipids

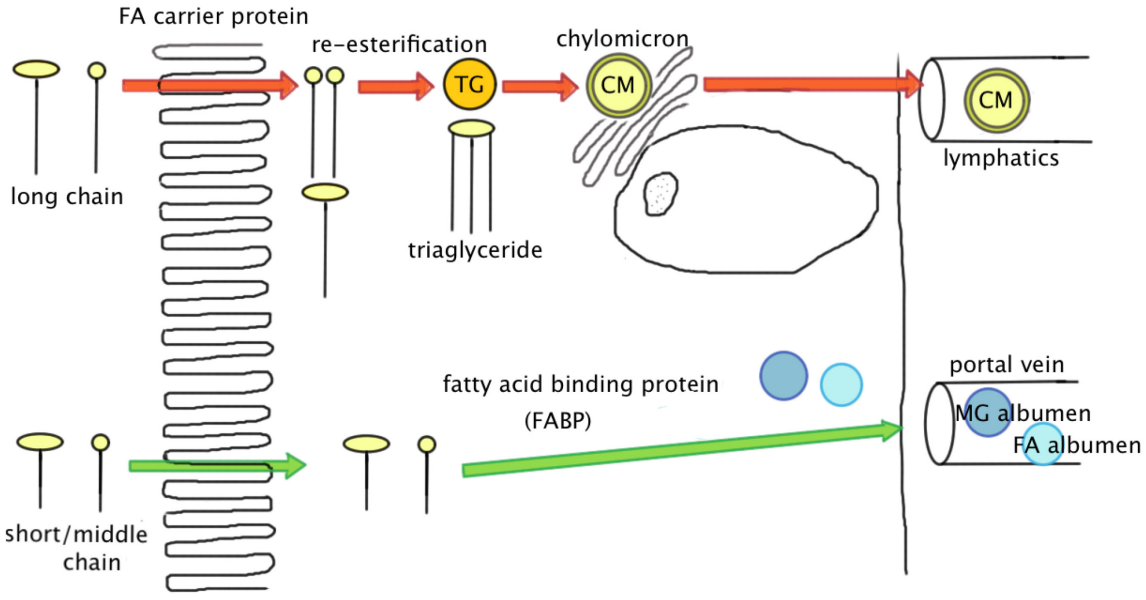


**Figure 3.** The schematic absorption pathways of lipid digestion products with different chain lengths

### 1.3. Intestinal drug absorption and lymphatic drug delivery

Once we know that the absorption of drugs or nutrient is largely dependent on lipid digestion and absorption, various lipid-based systems can be designed to facilitate lipophilic drug absorption. Some possible mechanisms of intestinal drug absorption with lipid-based formulations are summarized in **Fig. 4** (*7*)**,** including (A) increased membrane fluidity facilitating transcellular absorption; (B) opening of the tight junction to allow paracellular transport, mainly relevant for ionized drugs or hydrophilic macromolecules; (C) inhibition of P-gp and/or CYP450 to increase intracellular concentration and residence time; (D) stimulation of lipoprotein/chylomicron production. Among which, the last two mechanisms are the most promising for intestinal lymphatic drug targeting using lipid-based vehicles.

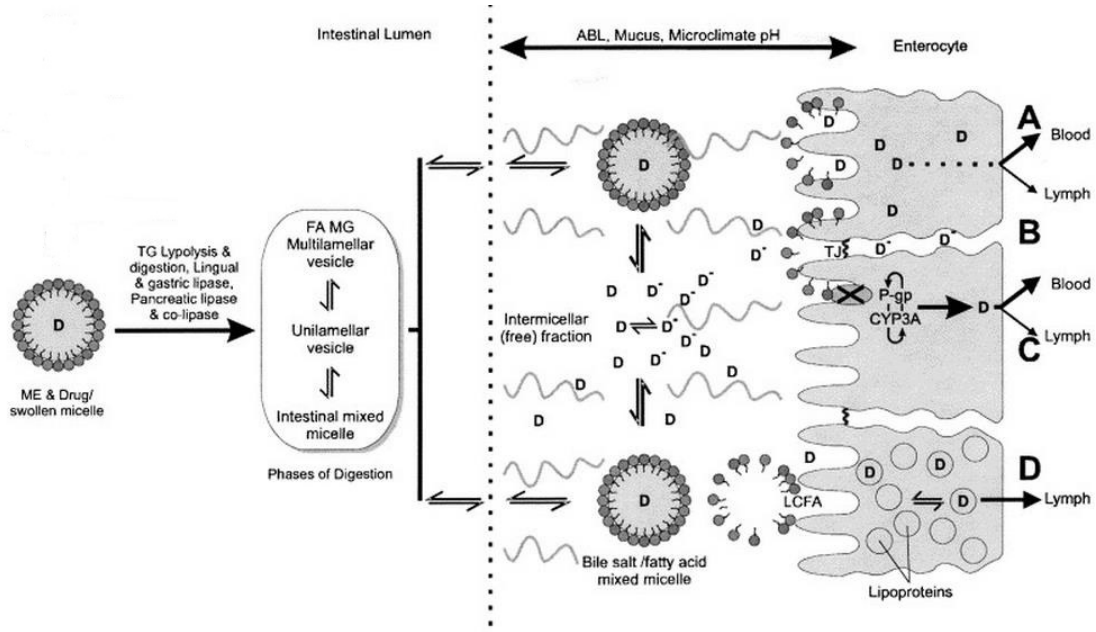


**Figure 4.** Mechanisms of intestinal drug transport from lipid-based formulations via the portal vein and lymphatic routes**.** ABL: aqueous boundary layer; D: drug; D $^{-}$: ionized drug; FA MG: fatty acid monoglyceride; LCFA: long chain fatty acid; ME:

microemulsion; TG: triglyceride; TJ: tight junction (Reprinted from **Ref. 7**)

As mentioned, many drugs that are absorbed from the intestine portal vein system undergo first-pass metabolism in the liver before entering into the systemic circulation, which results in a much lower bioavailability. On the other hand, some highly lipophilic drugs that have a log P value > 5 and a long-chain triglycerides solubility > 50 mg/g will possibly transport with the intestinal lymphatic system and avoid the first-pass effect (*23*). Moreover, since the dynamics of intestinal lymphatic transport can influence drug concentration and persistence in the lymphatic system and systemic circulation, the toxicity profile of drugs can be also be reduced (*24*). The comparison of the above mentioned two systems in drug transport can be summarized in **Table 1**.

**Table 1.** Comparison of portal vein and lymphatic drug transport

| Portal vein transport | Lymphatic transport |
|---|---|
| Higher flow rate (blood flow is 500 times higher than lymphatic flow) | Lower flow rate (lymphatic flow) |
| Small, lipophilic compounds | Small, highly lipophilic compounds; Large (>10 000 Da), or extremely hydrophilic compounds and large colloidal structures |
| Through fatty acids binding protein (FABP) in the form of micelles | Through TG re-synthesis into colloidal structures in the form of TG and CM |
| With middle/short chain FAs or lipids (<12-C) | With long chain FAs or lipids (12-C and above) |

Inspired from these principles, design of lipid-based, especially long chain lipid-based delivery systems in enhancing the lymphatic transport of lipophilic drugs and nutraceuticals provide the researchers the most promising targeting.

### 1.4. Lipid-based delivery systems for lymphatic drug delivery

The simplest approach to evaluate absorption of drugs from lipid-based systems is to suspend or dissolve the drug in the chosen lipid (*9*). However, with the development of modern technology, especially with nanotechnology being utilized in the food and drug formulation development (*25, 26*), it is now possible to further enhance the absorption of the drug by using more advanced delivery systems. Among these developed systems in the state of art, lipid-based nanoparticles can be used to overcome many of the drawbacks of conventional dosage forms, such as improving solubility and dissolution rate, increasing bioavailability, protecting sensitive drugs from degradation, and also reducing some side effects. Moreover, the nanoparticle formulations can also passively or actively enable targeting specific biological sites by modifying their surface (*27, 28*). In this section, several common lipid-based nanoparticle delivery systems in improving the lymphatic drug transport are briefly introduced.

#### 1.4.1. Nanoemulsions and microemulsions

Both nanoemulsions and microemulsions have similar structure and compositions, being a dispersed phase stabilized by surfactants or emulsifiers in the continuous phase. Usually, for the lipophilic drug and nutraceutical delivery, oil-in-water (O/W) system is the dominant form. Nano-/micro-emulsions are heterogeneous systems derived from the conventional emulsion but with some unique characteristics in size, stability or others (*29*). In common definition, both nanoemulsion and microemulsion have dispersed particle sizes (radius) smaller than 100 nm. Microemulsion is a thermodynamically stable system under specific environment, while nanoemulsion is not, which will tend to breakdown during certain time of storage (*30, 31*). However, microemulsion usually

contains much higher concentrations of surfactants/stabilizers in the system compared with nanoemulsion. Both of these two systems find themselves specific applications in drug/nutraceutical delivery by incorporating lipids with different chain lengths (*32-34*).

### 1.4.2. Self- (nano) emulsifying drug delivery systems

Self- (nano) emulsifying drug delivery systems (SEDDS) are isotropic mixtures of natural or synthetic oils, solid or liquid surfactants, or hydrophilic solvents and co-solvents/surfactants used for the improvement of oral absorption of highly lipophilic drugs (*35-37*). Upon mild agitation when diluted in aqueous media, such as GI fluids, SEDDS systems can form fine O/W emulsion or microemulsions due to the entropy change favoring dispersion is greater than the energy required to increase the surface area of the dispersion (*38*). If properly designed, these self-emulsifying formulations can spread easily in the GI tract, with the digestive motility of the stomach and intestine provides the agitation necessary for self-emulsification.

The oil represents one of the most critical excipients in the SEDDS formulation because it can not only solubilize lipophilic drug, but also increase the portion of lipophilic drug transported via the intestinal lymphatic system. Holm *et al.* (*39*) examined the oral absorption and lymphatic transport of halofantrine in cannulated canine model after administration in SEDDS containing structured triglycerides, and found a 17.9% lymphatic availability of halofantrine via the thoracic duct and produced a total bioavailability of 74.9%. Kommuru *et al.* (*40*) developed several different coenzyme $Q_{10}$ containing SEDDS with different oils and assessed their bioavailability in dogs. An improved bioavailability was observed in the SEDDS formulation compared with the powder form of the drug.

### 1.4.3. Liposomes

Liposome is a nano-sized biodegradable lipid vesicle with aqueous space surrounded by a lipid bilayer. The lipophilic drugs can be entrapped in between the hydrophobic tails region inside the bilayer structure. It has received considerable interest as a vehicle for drug lymphatic targeting, due to its ability to enhance the permeability of drugs across the enterocyte, to stabilize drugs, and to provide the opportunity of controlled release (*41-43*). Previous studies suggested that liposome delivered compounds were selectively transported into lymphatic tissue following intraperitoneal administration (*44, 45*), intramuscular (*46*) or subcutaneous (*47*) injections. Also, the lymphatic uptake of liposomes of various sizes, lipid compositions and surface characteristics were investigated, and reported to be important for the lymphatic drug delivery (*48-50*).

### 1.4.4. Solid Lipid Nanoparticles

Solid lipid nanoparticles (SLN) is an alternative carrier system to traditional colloidal systems as mentioned above. The structural comparison of a SLN and a lipid nanoemulsion is shown in **Fig. 5** (*51*). Although with similar structure like O/W emulsion, SLN is made from lipids with high melting point, which remains in the solid state at room and body temperatures. Lipids used for SLN are typically physiological lipids, including fatty acids, steroids, waxes and mono-/di-/tri-glycerides mixtures. The use of these crystallized lipids can increase control over release and stability of incorporated drugs and bioacitves due to the mobility of the compounds in the solid matrix is minimized (*52, 53*).

SLN, since its first introduction around two decades ago, has gained increased

attention in pharmaceutical, food and cosmetic industries (*54-57*). It combines the advantages of traditional systems but avoids some of the major disadvantages in protecting labile drug from degradation in the body and for sustained release. The lipid core of the solid lipid nanoparticle can also stimulate the formation of chylomicrons, which transport the carrier and associated drug via the classical transcellular mechanism of lipid absorption, and thus promote the lymphatic drug delivery (*58-60*). Moreover, since the solid lipids (long chain fatty acids) in SLN are relatively difficult to be digested by the lipase in GI tract, a great portion of SLN can even be absorbed intactly without releasing of encapsulated compounds. It has been reported that after intraduodenal administration of SLNs for rats, they can get into the lymphatic system with intact structure (*61*).

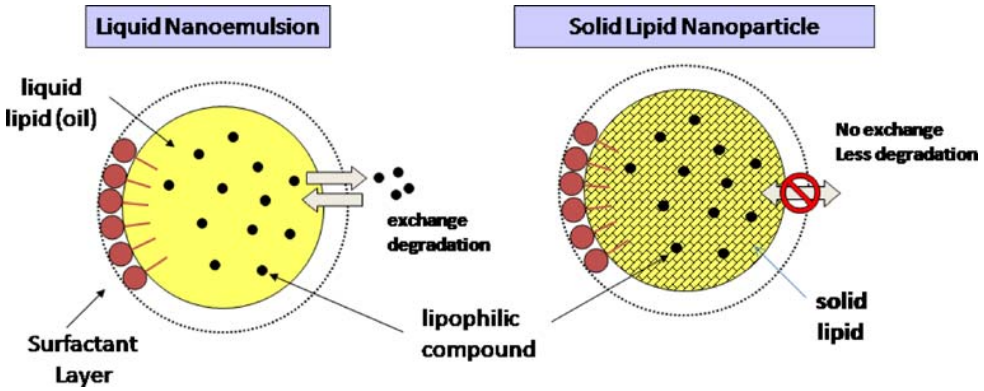


**Figure 5.** Structure comparison of nanoemulsion (left) and solid lipid nanoparticle (right) carrying a lipophilic compound (Reprinted from **Ref. 51**)

The superior uptake of methotrexate through the lymphatic system and into the systemic circulation has been demonstrated in methotrexate-loaded SLNs (*60*). In this study, the effect of different lipid-based SLNs was investigated by intraduodenal

administration. A 10-fold increase of methotrexate concentration was observed in the lymphatic system with methotrexate-loaded SLNs compared with methotrexate solution. Aji Alex *et al.* (*62*) designed glyceryl behenate based SLNs for the intestinal targeting delivery of lopinavir, and proved that SLN increased the cumulative percentage dose of lopinavir secreted into the lymph, with a 4.91-fold higher than a conventional drug solution. These results together with other evidences indicate that SLNs could be an excellent drug delivery system that improves the lymphatic delivery and overall bioavailability of lipophilic drugs.

### 1.5. Models to study intestinal lymphatic transport

#### 1.5.1. *In vivo* models

Evaluation of intestinal lymphatic drug transport cannot be performed directly in human studies, since it requires invasive and largely irreversible surgeries to access and cannulate the intestinal lymphatic duct (*24*). Therefore, a number of animal models have been developed to assess the intestinal lymphatic drug transport, and to estimate the overall drug absorption (*63*).

The majority of lymphatic transport studies reported was performed on cannulated rats, due to relative ease of operation and housing of this small animal in the laboratory. Among which, the triple cannulated rat model (where the mesenteric lymph duct, jugular vein and duodenum are accessed) has been widely used for the assessment of lymphatic transport in both anaesthetized and conscious models (*64, 65*). This model collects the entire volume of lymph flowing through mesenteric or thoracic lymph duct cannulas and therefore provides an absolute indication of the extent of lymphatic transport. Also, besides the rat model, other models by using larger animals like dogs (*66-68*), pigs (*69*),

sheep (*70, 71*) and rabbits (*72*) have also been described.

In addition to the traditional cannulated model, other models have also examined the use of a lympho-venous shunt, which allows sampling of lymph over a much longer period, thus enables the analysis of drug concentrations in lymph at fixed time intervals (*73*). While the limitation of this model will be the difficulty in estimating the absolute extent of lymphatic transport with relatively small database for lymph flow rates. More recently, an alternative *in vivo* approach (an indirect method) to estimate intestinal lymphatic drug transport has also been developed. It assesses the systemic exposure of drugs after administration in the presence or absence of an intestinal chylomicron flow inhibitor (e.g. Pluronic-L81 or colchicine) (*74*). The merit of this model is obviously to avoid surgical intervention, and provide more rapid screening. However, the broader implications of chylomicron flow blocking and intestinal lipid processing on drug exposure and lymphatic transport still need to be further studied in details.

### 1.5.2. *In vitro* models

The use of *in vitro* models for the assessment of lymphatic drug transport is also worth mentioning. Although not being able to fully reflect the real situation of lymphatic drug transport occurred *in vivo*, it still provides useful information related with the mechanisms and other influencing factors associated with the degree of lymphatic transport.

Among available *in vitro* models, the Caco-2 cells can be employed as a most prospective cell line to examine the influence of lipid and lipidic excipients on drug incorporation into lipoproteins and lymphatic transport due to its ability to secrete

lipoprotein, including chylomicrons. In the presence of fatty acids, Caco-2 cells can produce the triglyceride-rich lipoproteins of similar size and density to those synthesized by the human intestine. Ven Greevenbroek *et al.* found that Caco-2 monolayers will secrete low density lipoprotein (chylomicrons) or very low density lipoproteins (VLDLs) when exposed to long chain unsaturated fatty acids, such as oleic (18:1) and linoleic (18:2) acids. While, on exposure to saturated fatty acids, secretion of intermediate to low density lipoprotein predominated. Moreover, the lipoprotein secretion by Caco-2 cells is also affected by carbon chain length and position of the double bonds (*75-78*). Similar trends also have been reported in several *in vivo* studies (*79, 80*) indicate good *in vitro* and *in vivo* correlations (IVIVC), and reliable reference of this cell culture model.

**1.6. Vitamin E and delta-tocopherol**

Vitamin E is the most important fat-soluble antioxidant in human and animal tissues (*81*). Chemically, it is a group of compounds that have a phenolic functional group on the chromanol ring with an attached isoprenoid side chain (*82, 83*). It consists of tocopherols, which have a 16-C, saturated side chain, and tocotrienols with have the same 16-C chain, but with three unsaturated bonds. Both the tocopherols and tocotrienols have 4 homologues (alpha, beta, gamma, and delta); with differences in the number or location of methyl substituents in the chromanol ring (**Fig. 6**) (*84*).

Among all the derivatives of vitamin E, gamma and alpha tocopherol (γ-, α-T) are the major dietary tocopherols present in the human diet. And traditionally, α-T is the most studied one due to its superior activity in the classical fertility-restoration assay and its higher blood and tissue levels over other tocopherols and tocotrienols (*85*). For its health related activities, especially cancer-preventive effect, many studies have shown

that a lower vitamin E nutritional status is usually associated with increased risk of certain types of cancers (*86-88*). While some large-scale human trials with α-T failed to show any effect (*89-91*). Recently, the novel biological activities of other tocopherols, such as γ-T and δ-T, as well as tocotrienols, have been recognized (*92, 93*). Li *et al.* (*93*) reported δ-T is more active than other forms of tocopherols in inhibiting lung tumorigenesis in a mouse model. Guan *et al.* (*94*) concluded that δ- and γ-T, but not α-T, can inhibit colon carcinogenesis from the results of azoxymethane-treated rats.

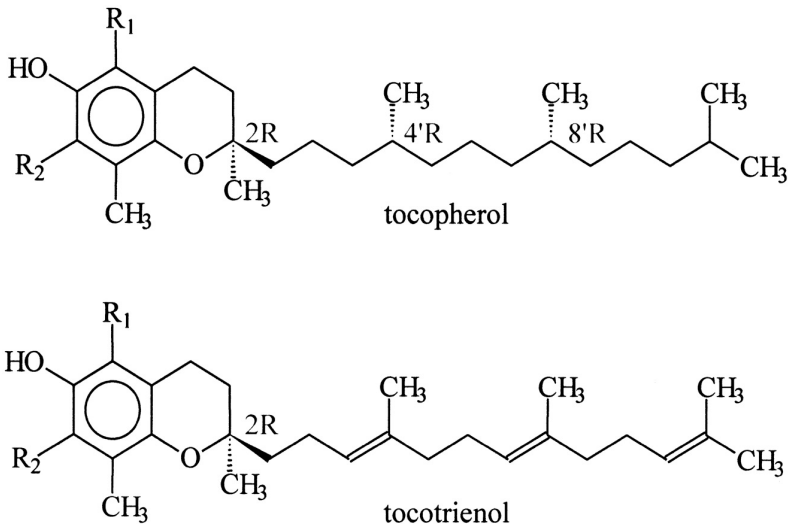


| $R_1$ | $R_2$ | |
|---|---|---|
| $CH_3$ | $CH_3$ | α |
| $CH_3$ | H | β |
| H | $CH_3$ | γ |
| H | H | δ |

**Figure 6.** Chemical structures of tocopherol and tocotrienol analogs (Reprinted from **Ref. 84**)

The absorption of dietary vitamin E occurs in the intestinal mucosa as the free phenolic form. Tocopherols tend to be incorporated into the chylomicrons and transported via the lymphatic system with the help of co-administered lipids. However, after tocopherols enter into the liver, the transfer of tocopherols in the liver to the VLDLs is mediated by a specific α-T transfer protein (*95, 96*). The α-T transfer protein in the liver selectively transfers α-T to VLDLs. Therefore, α-T is readily to be secreted into the

systemic circulation and transferred to non-hepatic tissues. Other tocopherols, like γ-T and δ-T, with very low affinity for the α-T transfer protein, thus are difficult to be transported out of the liver to the blood and other tissues. As a result, most of them are metabolized in the liver and excreted in the feces and urine.

This gives researchers an insight of designing delivery systems for δ-T and γ-T, to avoid their hepatic uptake and metabolism by selectively transportation via the lymphatic system, and result with higher concentrations in targeting tissues.

**1.7. Polymethoxyflavones and nobiletin**

Polymethoxyflavones (PMFs) refer to a general group for flavones with two or more methoxy groups on the benzo-γ-pyrone ($C_6$-$C_3$-$C_6$) skeleton with a carbonyl group at the $C_4$ position (*97*). PMFs are mostly found in *Citrus* genus, particularly in the peels of sweet orange and mandarin (*98*). In recent years, PMFs are gaining high popularity in research interests due to their broad spectrum of biological activities, including anti-inflammatory (*99, 100*), anti-carcinogenic (*101, 102*), anti-atherogenic (*103, 104*), anti-diabetic (*105*) and anti-obesity (*106*) properties, etc. Another reason lies in the fact that the major source of PMFs is orange peel, which is the byproduct of orange consumption. Therefore, the isolation and characterization of PMFs from orange peel not only makes good use of waste materials, and also lead to new applications of these compounds in nutraceutical and pharmaceutical industries.

Up to now, there are more than twenty PMFs being identified and isolated from different tissues of citrus plants (*107*). Among which, nobiletin is one of the most abundant PMFs. Nobiletin, named after *Citrus nobilis*, has six methoxyl groups on the

flavone backbone distributed at the 5, 6, 7, 8- position of A-ring and 3', 4'- positions of B-ring (**Fig. 7**) (*108*).

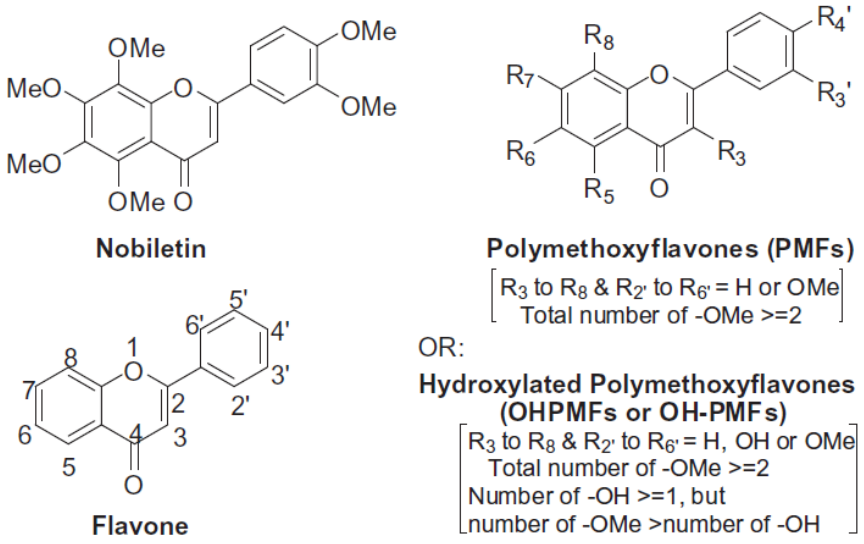


**Figure 7.** Chemical structure and nomenclature of PMFs, nobiletin and its derivatives (Reprinted from **Ref. 108**)

Besides inheriting the health beneficial activities like other PMFs, nobiletin can also notably ameliorate the memory impairment and Alzheimer's disease (*109-111*). However, clinical use of nobiletin is limited due to its poor solubility, bioavailability and fast metabolism. Moreover, the incorporation of nobiletin into pharmaceutical or nutraceutical related products are also hindered by the instability of the formulation and crystalline sedimentation (*112, 113*). Therefore, novel delivery systems in reducing the crystallinity and improving the stability and drug loading are highly demanded to improve the bioavailability of nobiletin and its related bioefficacies.

# CHAPTER 2: HYPOTHESIS AND OBJECTIVES

## 2.1. Hypothesis

Based on the above discussed background and rationale, I hypothesize that **by designing novel lipid-based delivery systems, the lymphatic transport and overall bioavailability of delta-tocopherol (δ-T) and nobiletin can be improved.**

## 2.2. Objectives

To test my hypothesis, I will pursue two specific objectives as listed.

**(I). Design novel SLN system for δ-T delivery, and investigate its *in vivo* effect in stimulating lymphatic transport of δ-T compared with other lipid systems.**

First of all, formulation design for δ-T loaded SLN with optimum configuration, processing condition and loading capacity will be determined. Then the physicochemical properties of δ-T loaded SLN will be characterized. More importantly, the effect of SLN in stimulating δ-T lymphatic transport will be determined and compared with a δ-T dispersion in corn oil, the prevalent dosage form of commercially available vitamin E and its related supplements for oral administration.

For the *in vivo* animal study, mice without cannulation will be used as the simple model to test and prove our hypothesis by accessing the levels of the target compound in tissues associated with either lymphatic or portal vein routes. Specifically, after oral ingestion of δ-T in different formulations, its levels in liver and blood will be analyzed to determine the fraction of δ-T transported via portal vein route. And δ-T levels in the thymus, the major lymphatic organ, will be determined to indicate the fraction of

lymphatic transport. The obtained results together with other supporting evidences will help to conclude whether or not SLN delivery system is better than corn oil in stimulating and improving the lymphatic delivery and overall bioavailability of δ-T.

**(II). Design novel nanoemulsion delivery system for nobiletin by reducing its crystallinity in the formulation, and investigate the effect of nanoemulsion in improving the bioaccessibility and permeability of nobiletin using *in vitro* models.**

Nobiletin is not easy to be incorporated into normal delivery systems with high loading and stability, due to its crystallinity and limited solubility in oil and aqueous systems. In my research, an O/W nanoemulsion system will be developed to enhance the solubility and reduce the crystallinity of nobiletin in the oil phase with the presence of cremophor EL (a polyethoxylated excipient). The developed nobiletin nanoemulsion formulation will be compared with an unformulated nobiletin suspension for the bioaccessibility determination by *in vitro* digestion model. Moreover, the permeation of nobiletin through the enterocytes will be simulated by the Caco-2 cell monolayer model, and compared between the formulated and unformulated forms. Results obtained from these *in vitro* models can tentatively indicate the improved bioaccessibility and bioavailability of nobiletin in the developed nanoemulsion formulation, if any. When necessary, *in vivo* animal tests will also need to be performed in the future.

# CHAPTER 3: DESIGN OF SOLID LIPID NANOPARTICLE DELIVERY SYSTEM FOR IMPROVED LYMPHATIC TRANSPORT OF DELTA-TOCOPHEROL

## 3.1. Introduction

Among various lipid-based delivery systems in the state of art, SLN with its superior advantages over other systems was chosen for the delivery of δ-T in current study. The comparison group we selected is δ-T dispersed in corn oil. The reason for choosing corn oil as the control is because most of the vitamin E related supplements currently available are in the form of mixture with vegetable oils (i.e. corn oil, sunflower oil, etc.), and filled in the softgels or capsules for oral use.

Corn oil is a mixture of different saturated and unsaturated long-chain fatty acids. Therefore, theoretically it can also promote the lymphatic transport of the lipid soluble vitamins and lead to an improved bioavailability. However, as mentioned in the earlier session, the chain length dependence of fatty acid absorption routes, either through intestinal lymphatic or portal vein, is not absolute. Likewise, for the drugs associated with lipids, its absorption route is also correlated with the chain length of the lipid vehicle and its own properties, but there is no clear cut either. Even though it is suggested that drugs with the long-chain lipid solubility > 50 mg/g, and log $P$ > 5 will possibly transport via the lymphatic route (*23*), still certain portion will be absorbed via the portal vein and hepatic route. However for δ-T, as we know, once transported into liver, it will be trapped with low chance to be further transported to other tissues. Therefore, the aim of this study, to be more specific, is to investigate whether SLN system performs better in bypassing the liver, and stimulating a higher proportion of the lymphatic transport of δ-T compared

with the traditional corn oil dosage form.

Due to the limitation of experimental resources and conditions, rather than some complicated models using cannulated rats or larger animals, we used mice without cannulation as the simple model to test and prove our hypothesis. The levels of δ-T in blood and tissues associated with either lymphatic or portal vein routes were accessed after the oral gavage of δ-T in tested formulations.

### 3.2. Materials and methods

#### 3.2.1. Chemicals and reagents

Compritol®888 (glyceryl behenate, m.p. 75 $^{o}$C) was obtained from Gattefossé (Paramus, NJ); d-α-forms of δ-tocopherol (containing 94% δ-T, 5.5% γ-T, and 0.5% α-T) was purchased from Sigma-Aldrich (St. Louis, MO). PC75, a phosphatidylcholine enriched lecithin was supplied by American Lecithin Co. (Oxford, CT). Corn oil purchased from a local supermarket was purified to remove any trace tocopherols before use. Sodium taurodeoxycholate (NaTDC) was purchased from CalBiochem (La Jolla, CA). Pancreatin with 8× USP specification and pepsin were purchased from Sigma-Aldrich (St. Louis, MO). Solvents for HPLC analysis were purchased from Pharmco-AAPER (Brookfield, CT). And other analytical chemicals and reagents were purchased from VWR International (West Chester, PA) and used without further purification and treatment.

#### 3.2.2. δ-T SLN preparation method

The δ-T loaded SLN formula was designed by using compritol® 888 as the solid lipid phase, and PC75 lecithin as the emulsifier. Hot melt emulsification method was

used to fabricate δ-T loaded SLN with the help of probe-ultrasonicator (Sonic dismembrator 550). Briefly, for each batch (10 g), 6 wt% (0.6 g) of solid lipids was melt at 85 $^{o}$C with hot plate, and mixed with 1 wt% (0.1 g) δ-T. At the meantime, the aqueous phase of 3 wt% (0.3 g) PC75 in 90 wt% (9 g) DI water, was also stirred and heated to 85 $^{o}$C until all the lecithin were fully dispersed and temperature equilibrium was reached. Then, immediately upon transferring the aqueous phase into the oil phase, sonication (level 4) was applied to the system with a probe at "5s on and 3s off" mode for 5 minutes to facilitate the disrupting and emulsifying of the lipid droplets. After sonication processing, fine and stable particles will be produced. The SLN was then cooled down and stored under room temperature until use.

### 3.2.3. δ-T SLN particle size measurement

The mean particle size and size distribution of the fabricated δ-T SLN were measured using a dynamic light scattering (DLS) based BIC 90 plus particle size analyzer equipped with a Brookhaven BI-9000 AT digital correlator (Brookhaven Instrument Corp., New York). The light source is a solid-state laser operating at 658 nm with 30 mW power, and the signals were detected by a high-sensitivity avalanche photodiode detector. SLN samples were diluted 100× with DI-water and well mixed prior to the measurement to prevent multiple scattering effects. All the measurements were conducted in triplicate at a fixed scattering angle of 90$^{o}$ at 25 $^{o}$C. The mean diameter of SLN was determined by cumulant analysis of the intensity-intensity autocorrelation function, G (*q, t*).

### 3.2.4. δ-T SLN zeta-potential measurement

The zeta-potential measurement of the δ-T SLN was carried out using a microelectrophoresis instrument (ZetaSizer Nano, Malvern Instrument) available at the

Center for Advanced Biotechnology and Medicine, Rutgers University. The ζ-potential value was calculated from the electrophoretic mobility of droplets in an applied oscillating electric field using laser Doppler velocimetry. SLN samples were diluted 100× with pH 3 and pH 7 buffers in disposable capillary cells. Measurements were performed in triplicate.

### 3.2.5. δ-T SLN structure characterization

The structure and morphology of the fabricated δ-T SLN were observed with transmission electron microscope (TEM). In this study, a JEOL 1230 TEM at Rutgers University was used to study the morphology of δ-T SLNs. The SLNs were dispersed directly into copper grid and stained by 1 wt. % phosphotungstic acid (PTA) solution. After drying under room temperature, samples were taken for TEM measurement.

### 3.2.6. δ-T SLN Gastrointestinal stability test

To mimic the effect of gastrointestinal environment (pH and enzyme) on the stability of δ-T SLN, an *in vitro* fed-state digestive lipolysis model was used to treat the SLN as described previously (*114*). In brief, the δ-T SLN was treated with simulated gastric fluid (SGF) followed by simulated intestinal fluid (SIF). The pH value for the SIF condition was kept at constant by adding alkaline (NaOH) to neutralize the liberated fatty acids from triglyceride digestion. After treatment, the content of digested lipids can be calculated according to the NaOH consumed. As a result, the undigested lipids referring the percentage of stable SLN can also be calculated to indicate its stability after going through the GI tract.

In specific, the δ-T SLN was first adjusted to pH 2 by HCl, and treated with SGF

composed of 40 mg/mL pepsin in 0.1 M HCl. After 30 min stirring under 37 $^{o}$C, it was adjust to pH 7.5 and transferred to a SIF solution that was composed of Tris maleate, NaCl, $CaCl_2 \cdot H_2O$, NaTDC, and phosphatidylcholine in concentrations of 50, 150, 5, 20, and 5 mM, respectively, mimicking the high concentrations of bile salts and endogenous phospholipids in the small intestine lumen. Pancreatin solution was prepared and added to initiate intestinal lipolysis under constant mixing. During a 2 h simulated digestion, the system pH was kept at 7.50 ± 0.02 by adding 0.25 mol/L NaOH at 37 °C. The NaOH concentration *vs.* time was recorded throughout the experiment, and the total NaOH consumed was obtained for final calculation.

### 3.2.7. Animal test

Animal experiments were performed under protocol no.02-027 approved by the Institutional Animal Care and Use Committee at Rutgers University. Mice were purchased from Jackson Laboratories (Bar Harbor, ME), and housed at the animal room under controlled temperature (20 ± 2 $^{o}$C), humidity (50 ± 10%), and 12 h light/dark cycles. A semi-purified AIN-93M diet was used to feed the mice. For the experiment, mice were randomly divided into two groups. The control group was fed with δ-T in corn oil, and the experimental group was fed with δ-T SLN, at the same δ-T dosage (8 mg δ-T / mouse). After gastric intubation with the δ-T formulations, mice were sacrificed by $CO_2$ asphyxiation at each predetermined time points (0, 0.5, 1, 2, 3, 4, 6, and 24 h). It was 5 mice per time point per group. Blood was then collected by cardiac puncture immediately before necropsy. Serum was collected by centrifugation of the blood samples at 3,000 g for 15 min, and frozen at -80 $^{o}$C until analysis. Relevant tissues were also collected, washed with saline before analysis. After 24 h, the δ-T levels in fecal samples of each

group were also collected and determined.

The δ-T levels in serum and tissues were measured by a method modified form a previously described procedure (*115, 116*). In brief, δ-T was extracted from 150 μL of plasma with ethanol and hexane, and then dissolved in a mixture of ethanol and acetonitrile. A HPLC system was developed using a Supelcosil C18 reverse-phase column, 5 μm (4.6×150 mm) with ethanol: acetonitrile (45:55) as the mobile phase. A waters 490 multi-wavelength detector (Water-Millipore) was used to detect absorbance at 292 nm.

### 3.2.8. Statistical analysis

All experiments data were expressed as means ± standard deviations. Where appropriate, data were analyzed using t-test by SigmaPlot 12.0 software, significant difference was defined at $p < 0.05$.

## 3.3. Results and discussion

### 3.3.1. Optimization of δ-T SLN preparation condition

In our designed δ-T SLN system, compritol® 888, a high melting point lipid with long-chain fatty acids (22-C) widely used for sustained release of oral solid dosage was chosen as the lipid phase. PC75, a phosphatidylcholine enriched lecithin together with other fractions of phospholipids, was selected as the emulsifier due to its excellent surface active property and natural source. Moreover, based on our previous experience, the ionic surfactant PC75 should produce charged droplets under wide ranges of pH conditions and contribute to the stability of particles (*117*).

For the formulation design and optimization, the content of δ-T in the SLN was

first fixed at 1 wt%, and 3 wt% of PC75 was dispersed in aqueous phase. The effect of solid lipid content and ultrasonic processing time on the produced δ-T SLN was optimized. First of all, we set the ultrasonic processing time for 3 min (level 4), and studied the influence of lipid contents on the mean particle size of δ-T SLN (**Fig. 8**). From the obtained data, there was a significant increase in the mean particle size when we increased the lipid content from 6% (235.2 nm) to 7.5% (267.7 nm). Therefore, 6 wt% of solid lipid was chosen for further use.

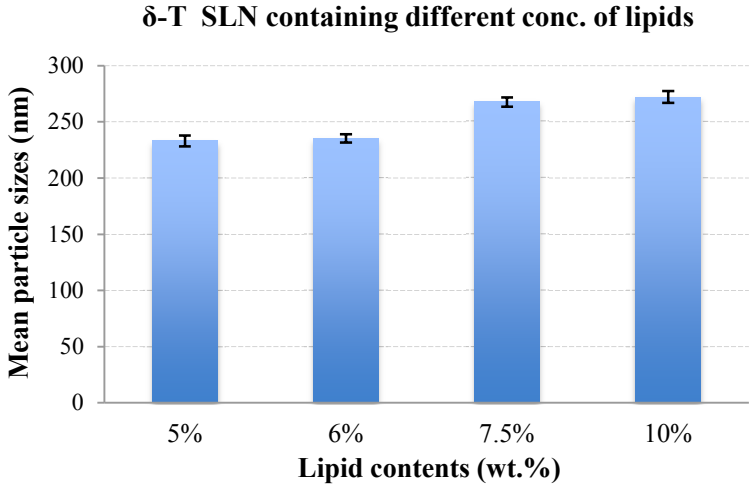


**Figure 8.** Mean particle sizes of δ-T SLN with different lipid contents (ultrasonic processing time: 3 min at level 4)

Then the effect of ultrasonic processing time on the particle size yield of δ-T SLN was further studied with the optimized formulation: 1 wt. % of δ-T, 6 wt% compritol® 888, 3 wt% PC75, and 90 wt% DI-water. Different processing time (1, 3, 5, 7, 10 min) was applied, and the results were given in **Fig. 9**. Initially the mean particle size decreased as the ultrasonic processing time increased. However, after 5 min, no significant differences were observed.

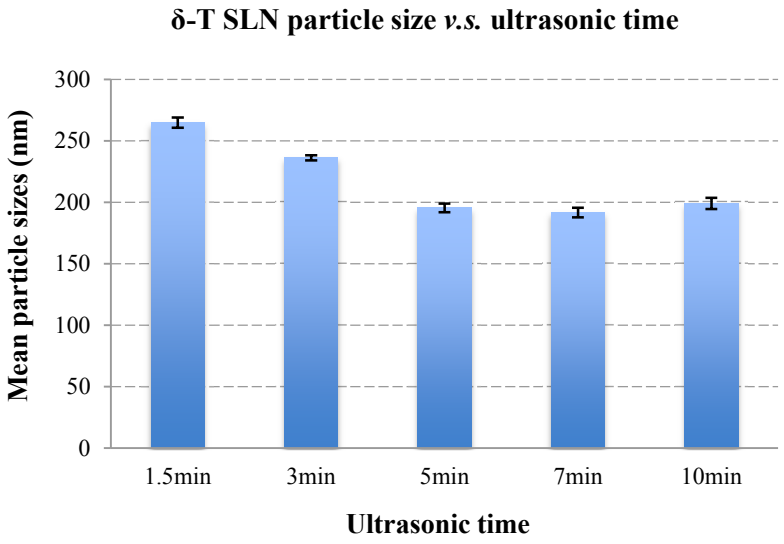


**Figure 9.** Mean particle sizes of δ-T SLN processed with different ultrasonication time

From the above trials, the formulation of δ-T SLN and the ultrasonic processing condition were determined as follows: 1 wt% of δ-T, 6 wt% compritol® 888, 3 wt% PC75, and 90 wt% DI-water, processed with 5 min of ultrasonication at level 4 using a Sonic dismembrator 550 system and hot melt emulsification method. The mean particle size of the δ-T SLN produced with the optimized formulation and processing condition was about 190 nm.

### 3.3.2. Zeta-potential measurement of δ-T SLN

The measurement of zeta-potential allows predication about the storage stability of colloidal dispersions. In general, the aggregation of particles is less likely to occur for charged particles due to the effect of electrostatic repulsion. In this study, zeta-potential values of the δ-T SLN in different pH conditions mimicking environments of the gastrointestinal tract were measured and listed in **Table 2**. In all tested pH conditions, the PC75 stabilized SLN showed negative-charged values, while decrease in zeta-potential

value was observed with decreasing of the pH values. The obtained results indicate strong electrostatic repulsion existed in between the SLN surfaces.

**Table 2.** Zeta-potential values of PC75 stabilized δ-T SLN under different pH conditions

| | pH 7 | pH 3 | pH 2 |
|---|---|---|---|
| zeta-potential (mV) | -51.6 ± 1.9 | -35.5 ± 0.8 | -18.7 ± 1.2 |

Moreover, the charge on the drug carrier particle is also an important factor in lymphatic uptake. It was reported that negatively charged carriers show higher lymphatic uptake than neutral or positively charged carriers due to the fact that the interstitial matrix contains a net negative charge (*118, 119*). In the interstitium, anionic carrier particles encounter electrostatic repulsion and move more quickly. While positively charged particles encounter more resistance to move towards due to the electrostatic attraction. Highly negatively charged (zeta-potential < -30 mV) particles have also been reported to be retained for a longer period of time in the lymph nodes (*118*). Therefore, PC75 stabilized SLN has the potential for improved lymphatic uptake.

### 3.3.3. Characterization of δ-T SLN morphology

A TEM study was carried out to examine the morphology of the produced δ-T SLN. In a typical δ-T SLN TEM image (**Fig. 10**) observed at the electron beam energy of 80 kV, sphere shaped particles were observed with intact structure, indicating the success of SLN production. And the particle sizes (in about 100-200 nm range) observed from TEM image also confirmed with the previous DLS data.

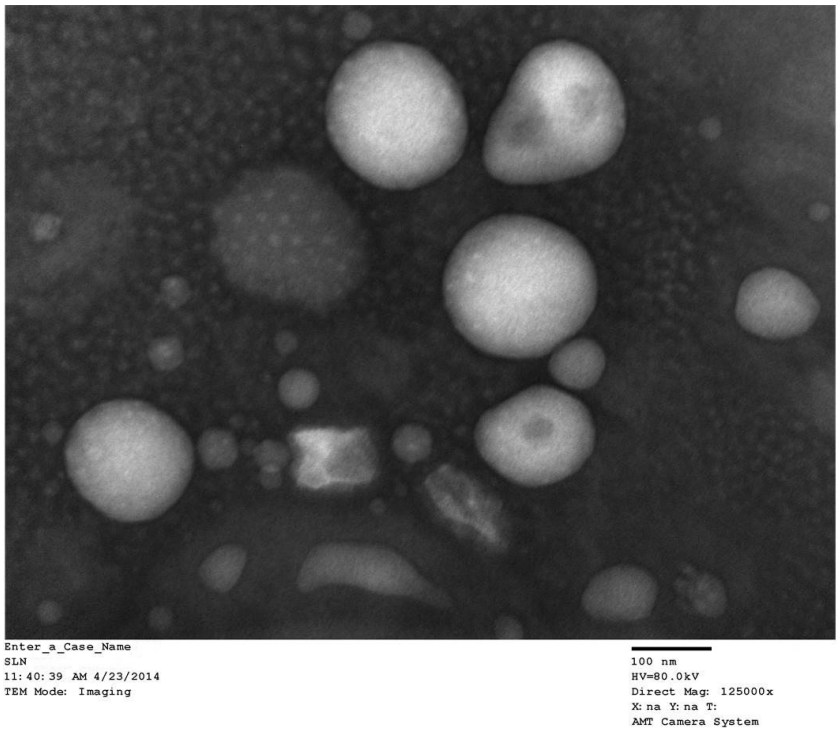


**Figure 10.** Transmission electron microscope image of δ-T SLN

### 3.3.4. Stability of δ-T SLN in simulated gastrointestinal environment

The stability of δ-T SLN was tested using an *in vitro* digestion model simulating both gastric and intestinal environments. After 30 min treatment in SGF, SLN was further exposed to SIF with pancreatic lipase to initiate lipolysis. According to stoichiometric ratio, it was assumed that upon lipase digestion, one mol of triglyceride released two mols of free fatty acids (FFAs) and consumed two mols of NaOH for neutralization to maintain the pH. The extent of lipolysis, defined as the percentage of triglycerides digested during lipolysis, may be determined from the total amount of NaOH consumed. A control was tested using a PC75 solution since lecithin may also generate FFAs by lipase and the amount of NaOH used for the mock lipolysis was subtracted. The following equation describes the calculation for extent of lipolysis:

$$\text{Extent of Lipolysis} = \frac{V_{NaOH}(t) \times C_{NaOH} \times M_{w,lipid}}{2 \times m_{lipid}} \times 100\%$$

where $V_{NaOH}(t)$ is the volume of NaOH titrated into the reaction vessel at the digestion time (t) to neutralize the FFAs released. $C_{NaOH}$ is the concentration of NaOH (mol/L), and $M_{w,\ lipid}$ is the average molecular weight of the lipid (g/mol). In this experiment, compritol® 888 has an average Mw of 1060 g/mol and $m_{lipid}$ is the total mass of digestible lipid added (g).

Based on the recorded results and calculation, we plotted the extent of lipolysis *vs.* the digestion time (**Fig. 11**). From the plot, only 12% of lipids in the SLN were digested after 120 min, indicating high stability of δ-T SLN in the GI tract. High fraction of undigested lipids also indicates possibility of intact structures remained for SLN after going through the digestive tract. To verify, the particle size profile of δ-T SLN after the lipolysis was also measured to compare with the pre-digestion data (**Fig. 12**). There was an increase in the mean particle size from 190 nm to 302 nm of δ-T SLN after the lipolysis probably due to the aggregation of some particles in the GI tract in response to the sudden change in pH and agitation. The intact structure of SLN particles, however, was still remained. Overall, our developed δ-T SLN showed good stability in the GI tract, and potential for the intact uptake.

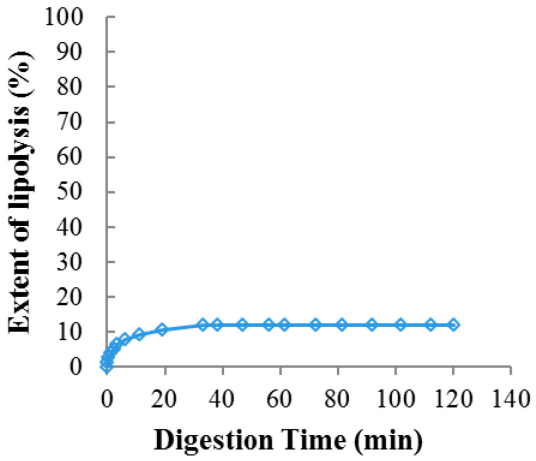


**Figure 11.** Extent of lipid digestion of δ-T SLN during a 2 hour *in vitro* lipolysis

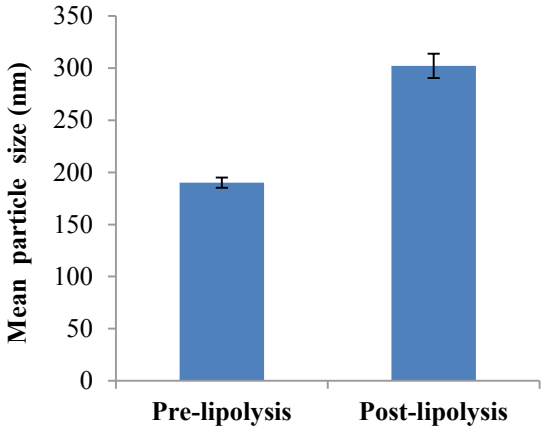


**Figure 12.** Mean particle size profiles of δ-T SLN before and after lipolysis

### 3.3.5. Levels of δ-T in blood

The monitoring of drug levels in blood after administration (pharmacokinetics curve) and the corresponding area under the curve (AUC) usually indicate the relative bioavailability of orally ingested drugs. In our study, however, they were used to indicate the proportion of drugs transported via the portal vein route directly into the systemic circulation. The levels of δ-T in mouse blood for up to 24 hours after feeding with same

dose of δ-T in both SLN and corn oil were determined and plotted in **Fig. 13**. From the plasma concentration profile of δ-T in corn oil group, there was an increase of δ-T leading to the plasma peak at approximately 2 h after administration. After this point, the concentration of δ-T showed a gradual decay over the time. However, for the δ-T in SLN, a much steadier curve with no obvious peak was observed. At 6 h after administration, the δ-T levels in two groups were similar. Unlike the decaying trend in the corn oil group, δ-T in the SLN group still showed similar concentration compared with the value at 4 h. Müller *et al.* (*120*) also reported the similar phenomenon that by using SLN as the drug carrier, it can avoid the initial plasma peak normally observed in other dosages forms, due to the prolonged release property of SLN. Moreover, this character will also help to alleviate the possibility of side effects, such as hepatotoxicity and nephrotoxicity.

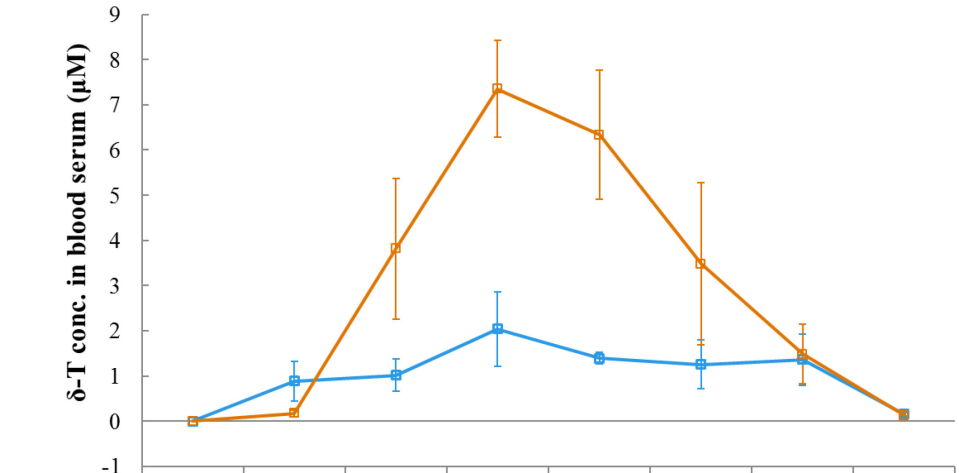


| | 0h | 0.5h | 1h | 2h | 3h | 4h | 6h | 24h |
|---|---|---|---|---|---|---|---|---|
| SLN | 0 | 0.887 | 1.019 | 2.038 | 1.39 | 1.254 | 1.359 | 0.156 |
| Corn oil | 0 | 0.175 | 3.817 | 7.353 | 6.334 | 3.480 | 1.487 | 0.126 |

**Figure 13.** Mean plasma profiles including standard variation (n=5) after oral administration of δ-T loaded SLN and corn oil

For the absolute δ-T levels in these two formulations tested, much lower plasma δ-T concentrations in SLN group were observed compared with corn oil group, especially at the early stage of absorption. However, due to the limitation of our experimental design, no data point was collected between 6 h and 24 h. It is possible that δ-T levels in SLN group might be slightly higher than the corn oil group somewhere between 6 h and 24 h. However it will not be contribute to AUC significantly. Overall, δ-T in corn oil group showed higher plasma levels and AUC compared with the SLN group. These results suggested that less proportion of δ-T in SLN was absorbed via the portal vein route into systemic circulation.

### 3.3.6. Levels of δ-T in livers

Liver is one of the largest glands in the digestive system, responsible for metabolism and other vital roles. All of the blood leaving stomach and intestine passes through liver. Then liver processes the blood and breaks down, balances, and creates nutrients for the body to use. Therefore, when drugs or nutrients are digested and transported via the portal vein route for absorption, liver is an inevitable stop before they can be further used for systemic circulation. However, many beneficial compounds are vulnerable for the hepatic metabolism (known as first-pass metabolism), which impairs their bioavailability to a large extent.

In this study, the δ-T levels in liver after administration was determined to indicate the proportion of δ-T transported via the portal vein route. From the obtained results (**Fig. 14**), higher levels of δ-T were found in the livers of mice fed with corn oil group at both 2 h and 3 h after administration. Significant lower δ-T levels, however, were detected in SLN group. Similar results also observed in later stage of absorption

(data not shown). These results of δ-T levels in liver also agreed with the previous determined δ-T levels in blood, indicating a less proportion of δ-T in the SLN was transported via the portal vein and hepatic route. On the other hand, whether the SLN can better promote the lymphatic transport will need to be proved.

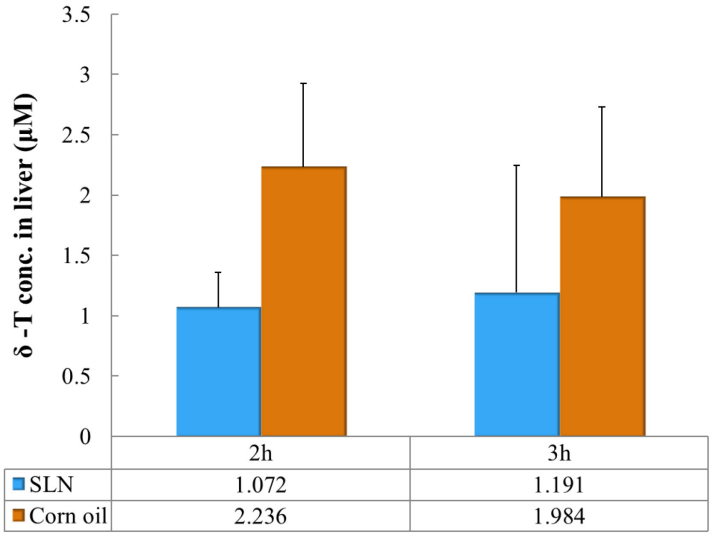


**Figure 14.** Concentrations of δ-T in mice livers after fed with δ-T containing SLN and corn oil at 2 h and 3 h

### 3.3.7. Levels of δ-T in thymus

Due to the limitation of the non-cannulated mice model, the entire volume of lymph flowing lymph duct cannot be determined to provide an absolute indication of lymphatic transport. A method of assessing δ-T in lymphatic tissues was used in this study to indirectly reflect the extent of δ-T transported via lymphatic route. Thymus, being a major lymphoid organ, was selected for study. The δ-T levels in thymus after administration of δ-T containing SLN or corn oil for 2 h and 3 h were determined and shown in **Fig. 15**. Significantly higher level of δ-T was detected in SLN group at 2 h compared with the corn oil group. And at 3 hours, an even huge difference (15× higher in

SLN group) was found. Data for 24 h (not shown) still showed an improved level of thymus δ-T in SLN. Therefore, we can tentatively conclude that SLN works better than corn oil in stimulating the lymphatic transport of δ-T.

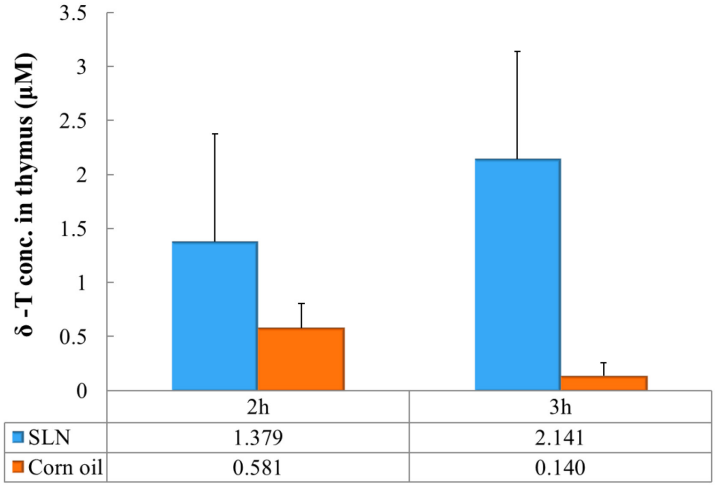


**Figure 15.** Concentrations of δ-T in mice thymus after fed with δ-T containing SLN and corn oil at 2 h and 3 h

### 3.3.8. Levels of δ-T in feces

Besides investigation of δ-T levels in either portal vein or lymphatic routes related blood or tissues, we were also interested to know the overall bioavailability of δ-T after administration of these two formulations. Theoretically, both the pharmacokinetic parameters and lymphatic absorption volume only partially reflect the overall bioavailability. While due to the difficulty and limitation of our experimental condition for measuring the absolute value of bioavailability, we determined the δ-T levels in feces collected during the 24 h of the two groups (**Fig. 16**), and used that as an indirect index for the overall bioavailability prediction.

From the results, a much higher level (7.8 ×) of δ-T was detected in feces samples

of corn oil group compared with SLN group. This result indicated a much lower amount of δ-T was excreted using SLN as the delivery system, thus a higher bioavailability can be achieved. Moreover, it also confirmed our findings of the superior advantage of SLN in promoting the lymphatic transport and circumventing the hepatic uptake and metabolism. Because once δ-T is transported to liver, there is a high likelihood of entrapment in the liver for metabolism or excretion due to lack of transfer protein.

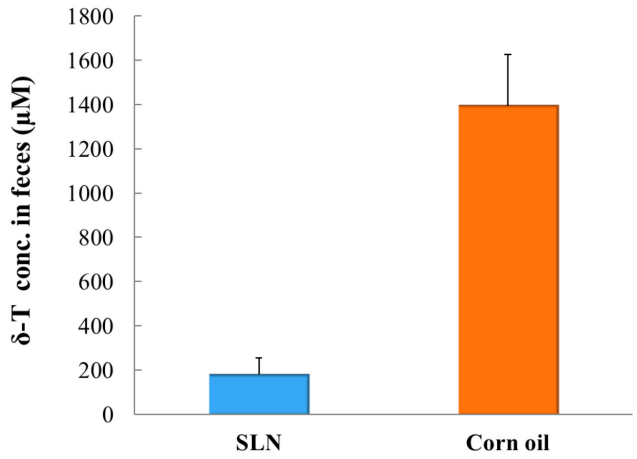


**Figure 16.** Concentrations of δ-T in mice feces accumulated during 24 h for both SLN and corn oil groups

### 3.3.9. Levels of δ-T in other tissues

We also had a chance to look into δ-T levels in other tissues that one may have interest. The δ-T levels in colon, skin, prostate, kidney, spleen, and fat (adipose tissue) were determined after 24 h of administration (**Fig. 17**). From the results, however, no significant differences were observed in most of the tissues. For some tissues, such as colon and kidney, slightly higher levels of δ-T can be found for the corn oil group. At current stage, we don't have a conclusive explanation for the observed results.

Theoretically, if the SLN can significantly promote the lymphatic transport and overall bioavailability compared with corn oil, higher levels of δ-T in most tissues should be observed. One possible reason may lies in the fact that process of intestinal lymphatic drug transport often continues over time periods much longer than typically observed for drug absorption via the portal vein. As a consequence, higher levels of δ-T in tissues might be achieved in a much prolonged time course than we've monitored for the SLN group.

Zara *et al.* (*121*) also reported less distribution of drug (idarubicin) in several tissues, such as heart, lung, spleen and kidney, when idarubicin was incorporated into SLN. Because the elimination half-life of idarubicin-loaded SLN was increased by 30-fold compared with idarubicin solution. Therefore besides stimulating the lymphatic transport of lipophilic drugs, SLN could be used to prolong the time course of drug delivery to the systemic circulation.

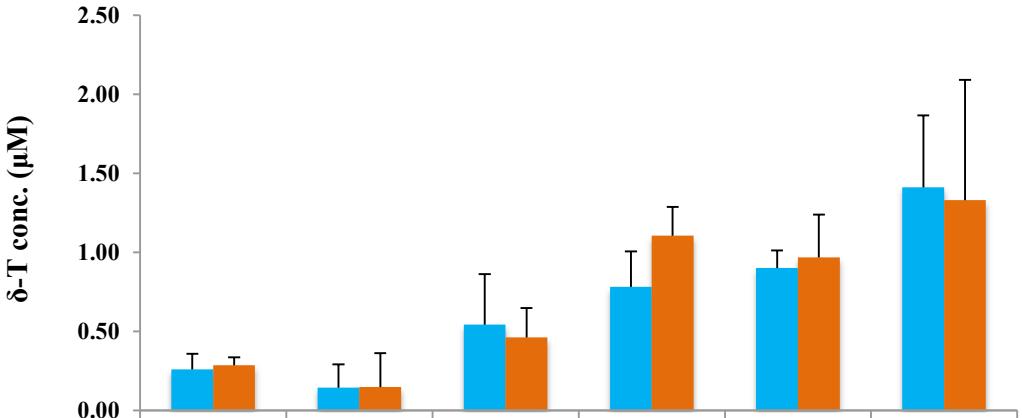


| | Colon | Skin | Prostate | Kidney | Spleen | Fat |
|---|---|---|---|---|---|---|
| SLN | 0.259 | 0.144 | 0.543 | 0.782 | 0.900 | 1.411 |
| Corn oil | 0.286 | 0.147 | 0.461 | 1.104 | 0.969 | 1.329 |

**Figure 17.** Concentrations of δ-T in colon, skin, prostate, kidney, spleen, and fat after 24 h administration of δ-T containing SLN and corn oil

### 3.4. Conclusion

A novel SLN was successfully developed with long chain lipid (compritol® 888), and anionic surfactant (PC75 lecithin) for δ-T delivery. The preparation conditions were carefully optimized. And the fabricated δ-T SLN was characterized with its particle size, morphology, zeta-potential, and gastrointestinal stability. Excellent physicochemical stability was observed.

The performance of the developed SLN in improving the lymphatic transport and overall bioavailability of δ-T were tested and compared in non-cannulated mice model with the control group, a dispersion of δ-T in corn oil. Lower δ-T levels detected in both blood and liver after administration suggested reduced occurrence of portal vein and hepatic transport of δ-T in the form of SLN. On the other hand, higher concentrations of δ-T were observed in thymus, a major lymphatic tissue, indicating improved lymphatic transport of δ-T with the SLN delivery system. The far less excreted δ-T level in feces further confirmed the improved lymphatic transport and overall bioavailability of SLN system. Moreover, SLN can prolong the release kinetics of δ-T and avoid the potential risk of toxicity in organs.

In conclusion, our study indicated that our developed SLN works better than corn oil in improving the lymphatic transport and overall bioavailability of δ-T.

# CHAPTER 4: DESIGN OF NANOEMULSION DELIVERY SYSTEM FOR REDUCED CRYSTALLINITY AND IMPROVED BIOAVAILABILITY OF NOBILETIN

## 4.1. Introduction

Nobiletin (NOB), one of most abundant polymethoxyflavones (PMFs), has a very low solubility in both water and oil phases at ambient temperatures. Therefore, it is easy to form crystals even in many oil-based delivery systems, such as regular O/W emulsion and SLN, when the loading exceeds its saturation level in the oil phase (*122*). This character greatly impaired its bioavailability and fortification in the pharmaceutical or functional food products.

Several recent studies have investigated the influence of oil types, emulsifier types, and processing conditions on the formation and stability of PMF-loaded O/W emulsion systems (*113, 122*). By properly designing of the emulsion system with optimized condition and configuration, the crystal of PMF can be inhibited to some extent. However, the problem still exists, and the achieved loading capacity of PMF in the emulsion was quite low. More recently, Ting *et al.* (*123*) designed a viscoelastic emulsion system for PMF and achieved high loading and stability with the help of the high viscosity of the formed emulsion. While the crystalline structure of PMF still largely exists, and the particle sizes were not small enough to define a nanoemulsion.

Therefore the aim of this this study is to design a nanoemulsion based delivery system for NOB. And achieve reduced crystallinity and high-loading capacity of NOB in the developed formulation. An excipient, cremopher EL-40 (polyethoxylated castor oil)

was introduced in the formulation to increase NOB's solubility and loading. NOB in our developed nanoemulsion system will be tested with *in vitro* digestion model and Caco-2 cell model for its bioaccessibility and transport efficiency compared with the unformulated form. Bioavailability improvement, if any, can be predicted form the obtained results.

## 4.2. Materials and methods

### 4.2.1. Chemicals and reagents

Nobiletin (>98% pure) was purchased from Quality Phytochemical LLC. (Edison, NJ). Neobee 1053 MCT was obtained from Stepan Co. (Northfield, IL). Cremopher EL-40 was provided by BASF Corporation (Florham Park, NJ). Sodium taurodeoxycholate (NaTDC) was purchased from CalBiochem (La Jolla, CA). Dimethyl sulfoxide (DMSO), pancreatin with 8× USP specification and pepsin were purchased from Sigma-Aldrich (St. Louis, MO). Caco-2 colon carcinoma cell line was obtained from Rutgers University. Penicillin and streptomycin, Dulbecco's modified eagle medium (DMEM), fetal bovine serum (FBS), MEM non-essential amino acid were purchased from Gibco (Grand Island, NY). 96-well cell culture plate, 12-transwell insets cell culture plate and other cell culture supplies were purchased from Corning Inc. (Corning, NY). Solvents for HPLC analysis were purchased from Pharmco-AAPER (Brookfield, CT). All other analytical chemicals and reagents were purchased from VWR International (West Chester, PA) and used without further purification and treatment.

### 4.2.2. NOB crystallinity observation

An inverted optical microscope (Nikon TE-2000-U) equipped with a charge-coupled device (CCD) camera (Retiga EXi, QImaging) was used for the NOB crystal

morphology observation. NOB oil suspension samples were directly monitored under the polarized light for the crystal morphology.

### 4.2.3. NOB-loaded nanoemulsion preparation

A NOB loaded O/W nanoemulsion was prepared by dispersing 0.5 wt% NOB in the 20 wt% MCT with the presence of 5 wt% cremopher EL-40 at heated condition (140 $^{o}$C) first. Upon the NOB was completely solubilized, the oil phase was mixed with the aqueous phase containing 4.5 wt% cremopher EL-40 as the emulsifier. The mixture was then processed with a high-speed homogenizer (Ultra-Turrax T-25 basic, IKA Works Inc.) at 24,000 rpm for 3 min followed by a high-pressure homogenizer (EmulsiFlex-C3, Avestin Inc.) at 100 MPa for 10 cycles at elevated temperature (70 $^{o}$C) condition. The fresh made emulsions were divided into three groups, stored at 4 $^{o}$C, 25 $^{o}$C, and 40 $^{o}$C, respectively, for the particle size and stability evaluation for 28 days.

### 4.2.4. Particle size measurement

The particle size of NOB-loaded O/W emulsion was measured using a ZetaSizer Nano ZS (Malvern Instruments) based on dynamic light scattering. NOB-emulsion samples were diluted 100 folds with DI-water before the measurements. Z-average size and size distribution profiles based on intensity were reported.

### 4.2.5. *In vitro* lipolysis model

The principle and recipe of lipolysis we used in this study are exactly the same as we described in last chapter for the *in vitro* digestion model. One can refer to sections 3.2.6 and 3.3.4 for details. Basically, upon digestion of triglycerides by lipase, the liberated free fatty acids were neutralized by NaOH of known concentration to maintain a

constant pH until the end of the reaction. Then the amount of NaOH consumed was used to back calculate the extent of digested lipids. However, rather than testing the stability of nanoemulsion against digestion, the aim of this study is actually to look at the bioaccessibility of nobiletin in the form of nanoemulsion after going through the GI tract. Because after digestion, certain percentage of nobiletin initially trapped in the lipid core will be liberated in the intestinal lumen, and become solubilized in the micelle structure formed by lipid digestion products together with endogenous bile salts and phospholipids. The solubilized nobiletin has the potential for the intestinal uptake and further utilization in the body. By definition, this solubilized fraction refers to nobiletin bioaccessibility.

### 4.2.6. NOB bioaccessibility determination

After lipolysis, the whole reaction liquid was ultracentrifuged at 4 °C and 50,000 rpm for 1 h (Ti 60 rotor, Beckman Coulter). The middle aqueous phase of micellar NOB was collected and filtered using 0.22 μm filters for concentration determination using HPLC. Then the total mass of solubilized NOB can be calculated by the product of the concentration of NOB in the aqueous phase and the total volume. And the corresponding nobiletin bioaccessibility can be calculated as follows:

$$\text{Nobiletin Bioaccessibility} = \frac{\text{Total mass of solubilized NOB}}{\text{Total mass of NOB input}} \times 100\%$$

### 4.2.7. Cell viability assay

Caco-2 cells were cultured in DMEM containing glucose and L-glutamine, supplemented with 10 % FBS, 0.1% MEM non-essential amino acid, 100 U/mL penicillin, and 0.1 % mg/mL streptomycin at 37 $^{o}$C in an atmosphere of 5 % $CO_2$ and 95 % air. The cells were split using trypsin/EDTA when 70-90 % of confluency reached.

Media was replaced every 2-3 days. The Caco-2 cells utilized in this study were between 38-50 passages. DMSO was used as the solvent to deliver NOB as the control group compared with NOB nanoemulsion. The final concentration of DMSO in all experiments did not exceed 0.1 %.

For the cell viability test, Caco-2 cells were seeded in 96-well plates at a density of 10,000 cells per well. After 12 h incubation, media was aspirated and experimental groups were treated with 100 μL culture media containing 1, 5, 15, 25, 50, 75, 100 μM of NOB in both DMSO and nanoemulsion forms. As the control, a separate group of cells treated with culture media only with no NOB was tested under same condition. After 12 h, the treatment media was replaced with 100 μL of complete culture media containing 0.5 mg/mL 3-(4,5-dimethylthiazol-2-yl)-2,5-diphenyltetrazolium bromide (MTT). Then, after 2 h incubation at 37 $^{o}$C, the media containing MTT was removed and the reduced dye was solubilized by addition of 100 μL of DMSO in each well. The absorbance at 570 nm for each well was determined using a spectrophotometric microtiter plate reader. Results were shown as percentage of viable cells in relative to the control group.

**4.2.8. Caco-2 cell transport assay**

Caco-2 cells were treated in the same condition as mentioned in the last section. The procedure of transport experiments with the cultured Caco-2 cells were performed according the protocol of a previous publication (*124*). Briefly, to generate Caco-2 cell monolayers in the insert filter of 12-well plates, 0.5 mL Caco-2 cells were seeded into the insert (the apical compartment) at the density of $6 \times 10^5$ cells/mL. Culture media in the lower (basolateral) compartment of each well was changed every 2-3 days, until 21-29 days of post seeding when a well-differentiated monolayer was formed. For monitoring

the transport of NOB through Caco-2 cell monolayer, the cultured Caco-2 cells were first washed twice by Hank's balanced salt solution (HBSS) and pre-incubated for 30 min. Then 25 μM NOB in both DMSO and nanoemulsion were added into the apical compartment to start the experiment. In the permeation direction of apical to basolateral (A-B) compartment, 0.4 mL donor media was added to the A-compartment and 1.2 mL receiving media was added to the B-compartment. Initial dosing solutions were immediately withdrawn from the apical compartment as reference for the initial concentration. Plates were then slowly shaken at 100 rpm at 37 $^{o}$C. At each 30 min interval up to 2 hours, samples from B-compartments were collected and the volume taken was replenished with HBSS.

**4.2.9. HPLC analysis of NOB**

All samples collected from the transport experiment were treated with ethyl acetate to extract NOB, and then gently dried by nitrogen blowing. The dried samples were re-solubilized by 100 μL of DMSO, and then subject to HPLC analysis. In this study, a Dionex HPLC system (Sunnyvale, CA) equipped with an UltiMate 3000 variable wavelength detector was used. And the column used for separation was an Ascentis® RP-amide $C_{18}$ (15 cm × 4.6 mm, 3 μm) from Supelco (Bellefonte, PA). The detection of NOB was carried out using gradient elution with the mobile phase of water (solvent A) and acetonitrile (solvent B) with the method developed previously (*125*). If brief, gradient elution started from 40% B linearly increased to 55% in 10 min, then increased to 70% in 5 min, until to 90% in another 1 min, and kept for 3 min. Then it was linearly decreased back to 40% in 1 min, and kept for 4 min for equilibrium. The flow rate was kept as constant at 1 mL/min. UV-Vis detection wavelength was set at 320 nm.

### 4.2.10. Statistical analysis

All data were expressed as the mean ± standard deviation. When appropriate, data were analyzed by SigmaPlot 12.0 software with a student t-test or one-way analysis of variance (ANOVA). Significant difference was defined at $p < 0.05$.

## 4.3. Results and discussion

### 4.3.1. NOB-loaded nanoemulsion design

To design a nanoemulsion delivery system for NOB, first is to choose the carrier oil. Three oils were taken into consideration in this study: MCT, corn oil, and orange oil. Based on previous reported data (*122*) and our own tests on the solubility of NOB in these three oils, MCT was finally chosen as the carrier oil, due to its highest solubility of NOB (ca. 1 mg/g) and less tendency of the crystal growing.

To achieve the increased NOB loading capacity in the carrier oil, an excipient is needed to largely improve the solubility of NOB and prevent its crystallization. Cremopher EL (CrEL), a polyethoxylated castor oil widely used in the pharmaceutical industry to solubilize hydrophobic drugs, came into our attention. It is a white to off-white viscous liquid with an approximate molecular weight of 3 kDa, and is produced by the reaction of castor oil with ethylene oxide at a molar ratio of 1:35 (*126*). With the help the CrEL, a much increased solubility was observed for NOB in the carrier oil. We were able to achieve the NOB solubility of ~25 mg/g MCT with the presence of 0.25 g CrEL. In order to reach our targeted NOB loading (0.5 wt%) in the final emulsion system, we set 20 wt% MCT as the oil phase in the formulation, and 0.5 wt% NOB was added in the oil phase together with 5 wt% of CrEL to get fully solubilized. The microscope pictures of NOB in MCT (25 mg/g) with and without CrEL were taken and shown in **Fig. 18**.

From the picture of NOB in MCT without CrEL (left), the loaded concentration was obviously supersaturated thus many needle-like NOB crystals were formed and tended to form clusters. While with the adding of CrEL as the excipient, all the NOB was solubilized in the oil phase with no crystal can be observed. These results proved the excellent effect of CrEL in improving the solubility and reducing the crystallinity of NOB in carrier oil system.

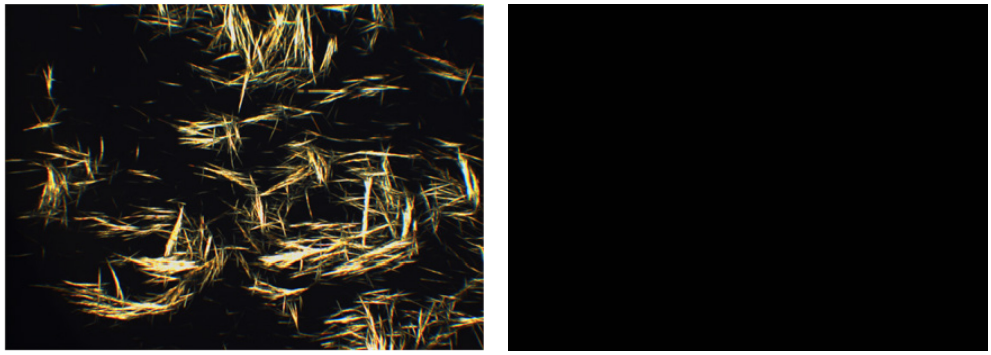

**Figure 18.** Polarized light microscope pictures of NOB in carrier oil MCT (25 mg/g) without (left) and with (right) CrEL

Next step is to select emulsifier for our O/W emulsion system. Due to the fact that CrEL itself is a non-ionic surfactant, therefore the emulsifying property of CrEL together with other three commonly used surfactants, i.e. whey protein isolate (WPI), lecithin (PC75), and modified starch (Purity Gum Ultra), were tested. Upon dissolving 0.5 wt% NOB in 20 wt% of MCT together with 5 wt% of CrEL, the aqueous phase containing 4.5 wt% of dispersed emulsifiers in 70 wt% of DI water was mixed with the oil phase. Then high speed and high pressure were applied under the conditions described in section 4.2.3 to produce O/W emulsions. The mean particle sizes of these fresh made NOB-loaded emulsions stabilized by different emulsifiers were determined as summarized in **Table 3**.

Among the obtained results, CrEL stabilized emulsion achieved smallest particle size and narrow size distribution (**Fig. 19**), therefore CrEL was selected as the emulsifier for the NOB-loaded emulsion.

**Table 3.** Mean particle sizes of NOB-loaded emulsions stabilized by different emulsifiers

| | CrEL | WPI | PC75 | Purity Gum Ultra |
|---|---|---|---|---|
| Mean Particle Size (nm) | 114.6 ± 5.2 | 186.7 ± 9.1 | 221.5 ± 11.8 | 747.8 ± 23.5 |

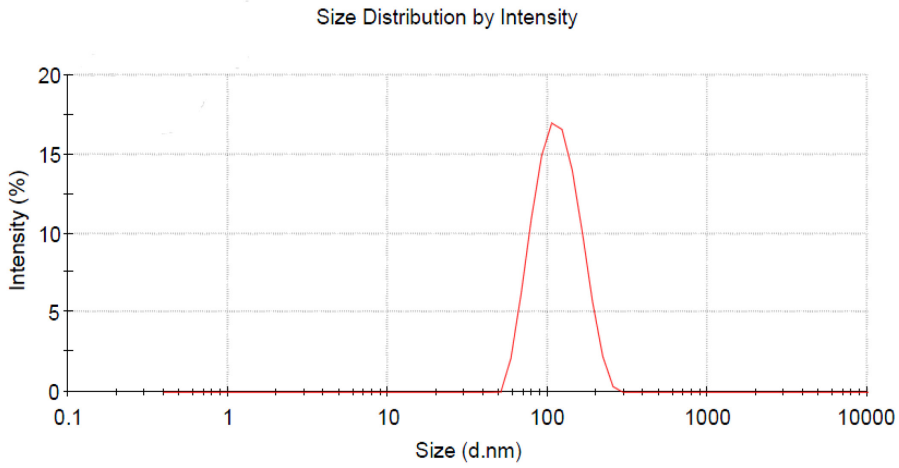


**Figure 19.** Particle size distribution profile of CrEL stabilized NOB-loaded emulsion

In summary, the formulation of NOB-loaded O/W emulsion was determined and optimized. A loading of 0.5 wt% NOB can be achieved in the nanoemulsion system consisting of 20 wt% of MCT together with 5% CrEL as the oil phase, and an extra 4.5 wt% of CrEL in 70 wt% of DI-water as the aqueous phase. The CrEL in the formulation functioned not only as an excipient to increase the solubility of NOB in the oil phase, but also as the emulsifier to stabilize emulsion. The produced emulsion had a nano-scale mean particle size (~115 nm), and narrow size distribution.

### 4.3.2. Physical stability of CrEL stabilized nanoemulsion

The physical stability of the CrEL stabilized nanoemulsion containing NOB was accessed by monitoring its particle size growing profiles under three different temperature storage conditions, i.e. 4 $^{o}$C, 25 $^{o}$C and 40 $^{o}$C, for 28 days. The obtained results were shown in **Fig. 20**. Superior emulsion stability was observed for the groups stored at 4 and 25 $^{o}$C conditions, with no significant growth of the particle sizes after 28 days. The elevated temperature condition (40 $^{o}$C) showed a relatively faster growth rate, probably due to the greater thermodynamic moving rate of particle, thus increased the possibility for droplets coalescence. Overall, all the emulsions showed excellent physical stability, no phase separation or precipitation was observed in all tested conditions during the storage period.

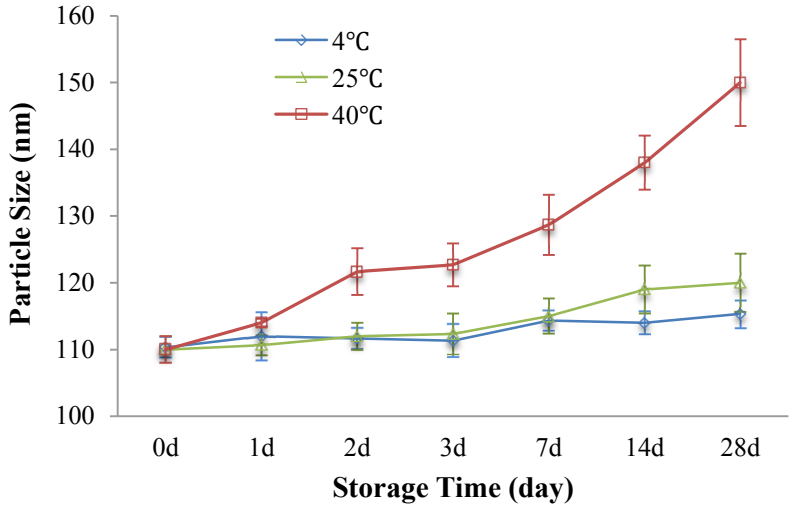


**Figure 20.** Particle size growth profiles of CrEL stabilized NOB nanoemulsion at 4 $^{o}$C, 25 $^{o}$C and 40 $^{o}$C for 28 days

### 4.3.3. *In vitro* bioaccessibility determination of NOB-loaded nanoemulsion

Bioaccessibility is the amount of a compound released from its matrix in the

gastrointestinal tract and become potential available for absorption. To access the bioaccessibility of NOB in the developed nanoemulsion, an *in vitro* digestion model based on lipolysis was employed. The extent of lipolysis of our developed NOB nanoemulsion, together with the comparison group, a NOB oil suspension, was tested during the 2 h digestion process. The digestion curves of both NOB nanoemulsion and oil suspension were plotted in **Fig. 21**. From the curves, almost complete digestion (~100%) of lipids in NOB nanoemulsion was observed after 2 h, contrasting with a 55% lipid hydrolysis in the NOB oil suspension. More importantly, the initial rate of lipid digestion was much faster for nanoemulsion than oil suspension. More than 60% of lipids were hydrolyzed in the first 5 min in the nanoemulsion, while only less than 10% being digested in oil suspension. The possible explanation for this observed result may lie in the fact that larger oil-water interfacial area of nanoemulsion droplets compared with the bulk oil phase and thus facilitates lipase hydrolysis.

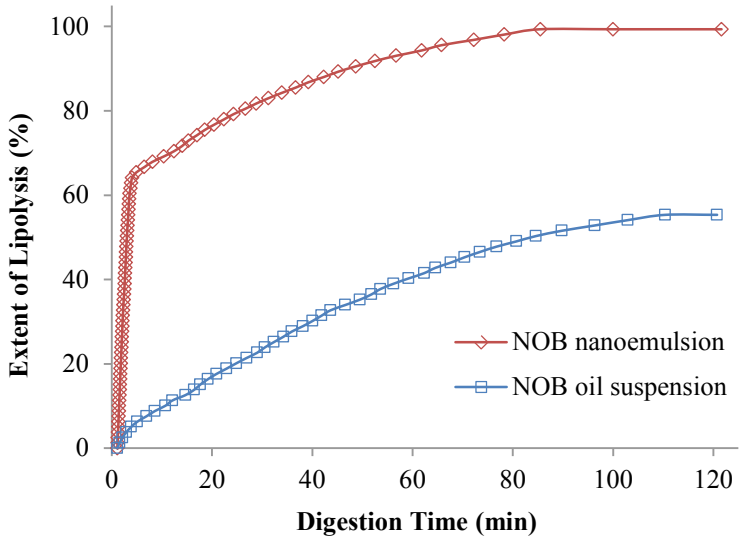


**Figure 21.** Comparison of *in vitro* lipolysis profiles of NOB nanoemulsion and NOB oil suspension

After the lipolysis, the bioaccessible fractions of NOB in both nanoemulsion and oil suspension were determined and shown in **Fig. 22**. Compared with the relative low bioaccessibility of NOB observed in the oil dispersion (23.6 %), a much increased level (84.1 %) was observed for our developed NOB nanoemulsion formulation. A nearly 4× increase was achieved in the current study. Since the bioaccessibility of a compound is a simplified but useful prediction for its oral bioavailability, our results indicated that the bioavailability of NOB can be significantly improved by designing O/W nanoemulsion delivery system.

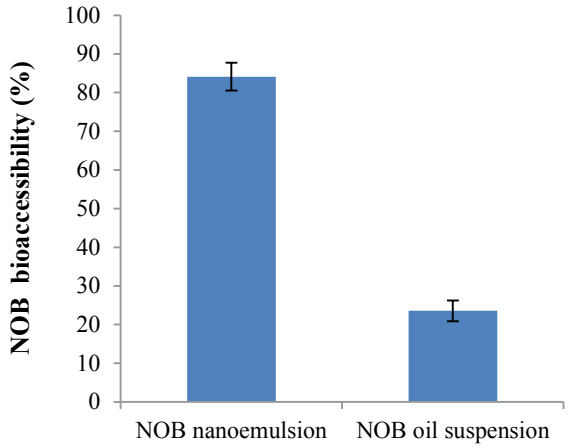


**Figure 22.** NOB bioaccessibility after lipolysis in both nanoemulsion and oil suspension

### 4.3.4. Cytotoxicity of NOB nanoemulsion

It has been reported that CrEL may modify the cytotoxicity profile when given concomitantly with certain anti-cancer agents (*126*). In order to investigate if the cytotoxicity of NOB will be changed in the form of nanoemulsion containing CrEL compared with the unformulated one in DMSO, the MTT assay using Caco-2 cell was conducted. From which, the appropriate concentration of NOB used for the transport

assay can also be determined.

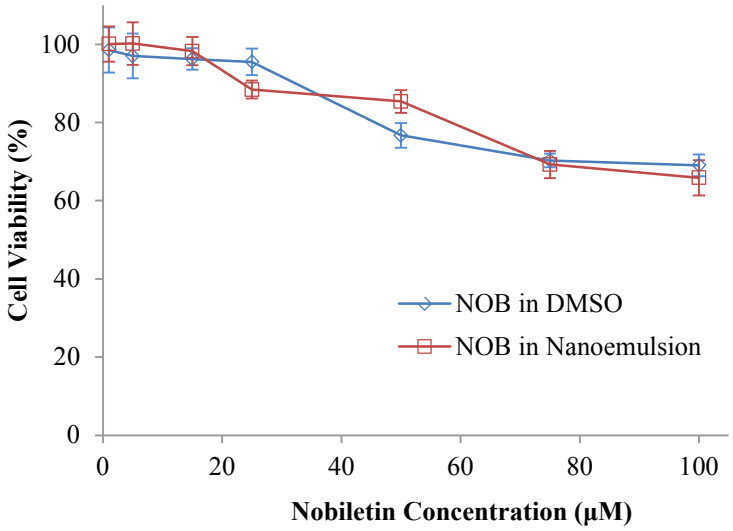


**Figure 23.** Effect of NOB (in nanoemulsion and DMSO) on the viability of Caco-2 human colon adenocarcinoma cells

From the results shown in **Fig. 23**, a gradual reduction trend of cell viability with increase of NOB concentration can be observed in both testing groups. Except for some variations at certain concentrations (25, 50 μM), no significant difference was observed for the anti-cancer effects of NOB in nanoemulsion and DMSO. Which means the presence of CrEL did not compromise the anti-cancer effects of NOB. Also, the results showed high cell viability in low NOB concentrations, while when concentration increased from 25 μM to 50 μM, cell viability will be reduced to lower than 80%. Therefore, 25 μM of NOB was selected for the subsequent Caco-2 permeation experiments.

### 4.3.5. Transport of NOB through Caco-2 cell monolayer

Once a compound becomes bioaccessible in the intestinal lumen, it has to further

permeate through the intestinal enterocytes and then be transported via either portal vein or lymphatics for potential utilization in the body. Therefore, studying the transport character of NOB will give us more information regarding its potential bioavailability. Caco-2 cell monolayers have been widely used to determine the permeation rate and to examine the permeation mechanisms of bioactive compounds (*127, 128*). It has been demonstrated that the *in vivo* absorption also be predicted from the apparent permeation rate ($P_{app}$) across the Caco-2 cell monolayers. Generally, a higher $P_{app}$ value indicates high absorption (*129, 130*). In this study, the $P_{app}$ values of NOB from apical to basolateral (A-B) in both nanoemulsion and DMSO were determined (**Fig. 24**). Results showed an average $P_{app}$ value of $5.5 \times 10^{-6}$ cm/s of NOB in the form of nanoemulsion, contrasting with the $P_{app}$ of $3.6 \times 10^{-6}$ cm/s for the NOB solubilized in DMSO. Therefore, a significantly improved permeation rate can be observed for NOB when it was dosed with our developed nanoemulsion formulation.

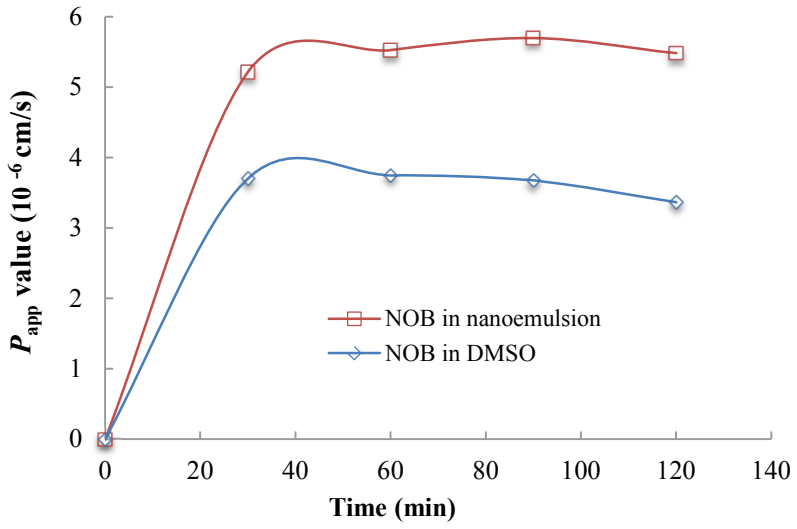


**Figure 24.** The apparent permeation rates ($P_{app}$) of NOB in nanoemulsion and DMSO determined by Caco-2 cell monolayer model

## 4.4. Conclusion

An O/W nanoemulsion delivery system was successfully developed for NOB. The addition of CrEL in the oil phase greatly increased NOB's solubility and reduced its crystallinity. Besides an excipient, CrEL also functioned as the emulsifier in the formulation and produced stable O/W nanoemulsion with small mean particle size (115 nm) and narrow size distribution. Excellent physical stability of the NOB-loaded nanoemulsion can be observed with no significant mean particle size change during storage. Moreover, a relatively high loading of NOB (0.5 wt%) with no crystalline structure can be achieved compared with regular lipid-based system.

The developed nanoemulsion was further tested with an *in vitro* digestion model to access the bioaccessibility of NOB in comparison with an unformulated NOB oil dispersion. Significantly higher percentage of bioaccessibility was achieved for the nanoemulsion (84.0 %) compared with the oil dispersion (23.6 %). From the MTT assay, no significant change of the cytotoxicity profile was observed for NOB in nanoemulsion and NOB dissolved in DMSO. And the transport experiment using Caco-2 cell monolayer further indicated the improved NOB permeation rate in the form of nanoemulsion ($P_{app}$ = 5.5 × $10^{-6}$ cm/s) compared with in DMSO ($P_{app}$ = 3.6 × $10^{-6}$ cm/s). From these *in vitro* results, it is predictable that NOB's *in vivo* bioavailability can also be greatly improved with our developed nanoemulsion formulation.

# CHAPTER 5: FUTURE WORK

Due to the limitation of time and conditions, still some meaningful experiments related with this thesis work were not able to be performed. However, they are worth mentioning and can be proposed as the future work for anyone who will be interested to further explore.

For the study of δ-T SLN lymphatic transport, it would be more informative to test on cannulated animal models for determination of the entire lymph volume flowing through lymph duct when resources are available. Our current experiments can only tentatively deduce the improved lymphatic transport of SLN in delivering δ-T compared with corn oil. While with more sophisticated animal models, an absolute extent of lymphatic transport can be indicated, and more solid conclusion can be drawn.

With the simple mice model as we used, a complete pharmacokinetics curve with more data points especially in the later stage should be obtained for future research to give a more comprehensive comparison of tested δ-T formulations. Additionally, for δ-T levels in all the tissues, a longer time course (> 24 h) after administration should be accessed, due to the fact that the process of intestinal lymphatic drug transport often continues over time periods much longer than the portal vein transport route. The SLN system has the property of prolonged release for its encapsulated compounds, which may contribute to a delayed accumulation in some tissues after oral administration.

For the study of reducing crystallinity and improving bioavailability of NOB, besides all the *in vitro* tests we performed, an *in vivo* study with animal model is strongly recommended to truly define the improved bioavailability of NOB in the developed

nanoemulsion formulation. Moreover, as this study didn't look into details about the lymphatic and portal vein routes for NOB absorption, a future study by using lipids with different chain lengths (MCT *vs.* LCT) in the emulsion systems can be performed. The correlation of lipid chain length with its absorption routes, and further implication on contributions to the overall bioavailability of NOB can be further determined. Last but not least, more novel delivery systems should be developed for NOB and other PMFs with similar characteristics to overcome the existing limitations, and make these beneficial compounds better delivered and utilized in our human body.

## REFERENCES


1. Louveau, A.; Smirnov, I.; Keyes, T. J.; Eccles, J. D.; Rouhani, S. J.; Peske, J. D.; Derecki, N. C.; Castle, D.; Mandell, J. W.; Lee, K. S.; Harris, T. H.; Kipnis, J., Structural and functional features of central nervous system lymphatic vessels. *Nature* **2015,** *523*, 337-341.
2. Yoffey, J. M.; Courtice, F. C., *Lymphatics, lymph and the lymphomyeloid complex*. London (& New York): Academic Press: 1970.
3. Cueni, L. N.; Detmar, M., The lymphatic system in health and disease. *Lymphatic research and biology* **2008,** *6*, 109-122.
4. Jerne, N. K., The immune system. *Scientific American* **1973,** *229*, 52.
5. Janeway, C. A.; Travers, P.; Walport, M.; Capra, J. D., *Immunobiology: the immune system in health and disease*. Current Biology Publications New York, NY;: 1999; Vol. 157.
6. Olszewski, W. L., The Lymphatic System in Body Homeostasis: Physiological Conditions. *Lymphatic Research and Biology* **2003,** *1*, 11-24.
7. O'Driscoll, C. M., Lipid-based formulations for intestinal lymphatic delivery. *European Journal of Pharmaceutical Sciences* **2002,** *15*, 405-415.
8. O'Driscoll, C. M., Anatomy and physiology of the lymphatics. In *Lymphatic transport of drugs*, Boca Raton, FL: CRC Press Inc: 1992; pp 1-35.
9. Humberstone, A. J.; Charman, W. N., Lipid-based vehicles for the oral delivery of poorly water soluble drugs. *Advanced Drug Delivery Reviews* **1997,** *25*, 103-128.
10. Porter, C. J. H.; Trevaskis, N. L.; Charman, W. N., Lipids and lipid-based formulations: optimizing the oral delivery of lipophilic drugs. *Nature Reviews Drug Discovery* **2007,** *6*, 231-248.
11. Shiau, Y. F., *Mechanisms of intestinal fat absorption*. 1981; Vol. 240, p G1-G9.
12. Bisgaier, C. L.; Glickman, R. M., Intestinal Synthesis, Secretion, and Transport of Lipoproteins. *Annual Review of Physiology* **1983,** *45*, 625-636.
13. Carey, M. C.; Small, D. M.; Bliss, C. M., Lipid digestion and absorption. *Annual Review of Physiology* **1983,** *45*, 651-677.
14. Thomson, A. B. R.; Keelan, M.; Garg, M. L.; Clandinin, M. T., Intestinal aspects of lipid absorption: in review. *Canadian Journal of Physiology and Pharmacology* **1989,** *67*, 179-191.
15. Tso, P., Intestinal lipid absorption. *Physiology of the gastrointestinal tract* **1994,** *2*, 1867-1908.
16. Fahy, E.; Cotter, D.; Sud, M.; Subramaniam, S., Lipid classification, structures and tools. *Biochimica et Biophysica Acta (BBA)-Molecular and Cell Biology of Lipids* **2011,** *1811*, 637-647.
17. Carrière, F.; Withers-Martinez, C.; van Tilbeurgh, H.; Roussel, A.; Cambillau, C.; Verger, R., Structural basis for the substrate selectivity of pancreatic lipases and some related proteins. *Biochimica et Biophysica Acta (BBA) - Reviews on Biomembranes* **1998,** *1376*, 417-432.
18. Hay, D. W.; Carey, M. C., Chemical species of lipids in bile. *Hepatology* **1990,** *12*, 6S-14S; discussion 14S-16S.

19. Lichtenstein, A. H.; Jones, P. J., Lipids: absorption and transport. In *Present Knowledge in Nutrition*, 2001.
20. McDonald, G. B.; Weidman, M., Partitioning of polar fatty acids into lymph and portal vein after intestinal absorption in the rat. *Quarterly Journal of experimental physiology* **1987,** *72*, 153-159.
21. McDonald, G. B.; Saunders, D. R.; Weidman, M.; Fisher, L., Portal venous transport of long-chain fatty acids absorbed from rat intestine. *American Journal of Physiology-Gastrointestinal and Liver Physiology* **1980,** *239*, G141-G150.
22. Bugaut, M.; Carlier, H., Role of intestinal hydrolases, endogenous substrates and chyloportal partition in fat absorption. *Fat Absorption* **1987,** *1*, 197-232.
23. Charman, W.; Stella, V., Estimating the maximal potential for intestinal lymphatic transport of lipophilic drug molecules. *International journal of pharmaceutics* **1986,** *34*, 175-178.
24. Trevaskis, N. L.; Charman, W. N.; Porter, C. J. H., Lipid-based delivery systems and intestinal lymphatic drug transport: A mechanistic update. *Advanced Drug Delivery Reviews* **2008,** *60*, 702-716.
25. Huang, Q.; Yu, H.; Ru, Q., Bioavailability and Delivery of Nutraceuticals Using Nanotechnology. *Journal of Food Science* **2010,** *75*, R50-R57.
26. Sozer, N.; Kokini, J. L., Nanotechnology and its applications in the food sector. *Trends in biotechnology* **2009,** *27*, 82-89.
27. Lembo, D.; Cavalli, R., Nanoparticulate delivery systems for antiviral drugs. *Antiviral Chemistry and Chemotherapy* **2010,** *21*, 53-70.
28. Kim, H.; Kim, Y.; Lee, J., Liposomal formulations for enhanced lymphatic drug delivery. *Asian Journal of Pharmaceutical Sciences* **2013,** *8*, 96-103.
29. McClements, D. J., *Food Emulsions: Principles, Practices, and Techniques, Second Edition*. Taylor & Francis: 2004.
30. McClements, D. J., Nanoemulsions versus microemulsions: terminology, differences, and similarities. *Soft Matter* **2012,** *8*, 1719-1729.
31. McClements, D. J.; Rao, J., Food-Grade Nanoemulsions: Formulation, Fabrication, Properties, Performance, Biological Fate, and Potential Toxicity. *Critical Reviews in Food Science and Nutrition* **2011,** *51*, 285-330.
32. Vyas, T. K.; Shahiwala, A.; Amiji, M. M., Improved oral bioavailability and brain transport of Saquinavir upon administration in novel nanoemulsion formulations. *International Journal of Pharmaceutics* **2008,** *347*, 93-101.
33. Gao, F.; Zhang, Z.; Bu, H.; Huang, Y.; Gao, Z.; Shen, J.; Zhao, C.; Li, Y., Nanoemulsion improves the oral absorption of candesartan cilexetil in rats: Performance and mechanism. *Journal of Controlled Release* **2011,** *149*, 168-174.
34. He, C.-X.; He, Z.-G.; Gao, J.-Q., Microemulsions as drug delivery systems to improve the solubility and the bioavailability of poorly water-soluble drugs. *Expert Opinion on Drug Delivery* **2010,** *7*, 445-460.
35. Shah, N.; Carvajal, M.; Patel, C.; Infeld, M.; Malick, A., Self-emulsifying drug delivery systems (SEDDS) with polyglycolyzed glycerides for improving in vitro dissolution and oral absorption of lipophilic drugs. *International journal of pharmaceutics* **1994,** *106*, 15-23.

36. Gursoy, R. N.; Benita, S., Self-emulsifying drug delivery systems (SEDDS) for improved oral delivery of lipophilic drugs. *Biomedicine & Pharmacotherapy* **2004,** *58*, 173-182.
37. Pouton, C. W., Formulation of self-emulsifying drug delivery systems. *Advanced Drug Delivery Reviews* **1997,** *25*, 47-58.
38. Reiss, H., Entropy-induced dispersion of bulk liquids. *Journal of Colloid And Interface Science* **1975,** *53*, 61-70.
39. Holm, R.; Porter, C. J. H.; Edwards, G. A.; Müllertz, A.; Kristensen, H. G.; Charman, W. N., Examination of oral absorption and lymphatic transport of halofantrine in a triple-cannulated canine model after administration in self-microemulsifying drug delivery systems (SMEDDS) containing structured triglycerides. *European Journal of Pharmaceutical Sciences* **2003,** *20*, 91-97.
40. Kommuru, T. R.; Gurley, B.; Khan, M. A.; Reddy, I. K., Self-emulsifying drug delivery systems (SEDDS) of coenzyme Q10: formulation development and bioavailability assessment. *International Journal of Pharmaceutics* **2001,** *212*, 233-246.
41. Gregoriadis, G.; Florence, A., Liposomes in Drug Delivery. *Drugs* **1993,** *45*, 15-28.
42. Lian, T.; Ho, R. J. Y., Trends and developments in liposome drug delivery systems. *Journal of Pharmaceutical Sciences* **2001,** *90*, 667-680.
43. Cai, S.; Yang, Q.; Bagby, T. R.; Forrest, M. L., Lymphatic drug delivery using engineered liposomes and solid lipid nanoparticles. *Advanced Drug Delivery Reviews* **2011,** *63*, 901-908.
44. Parker, R. J.; Hartman, K. D.; Sieber, S. M., Lymphatic absorption and tissue disposition of liposome-entrapped [14C] adriamycin following intraperitoneal administration to rats. *Cancer research* **1981,** *41*, 1311-1317.
45. Parker, R. J.; Priester, E. R.; Sieber, S. M., Comparison of lymphatic uptake, metabolism, excretion, and biodistribution of free and liposome-entrapped [14C] cytosine beta-D-arabinofuranoside following intraperitoneal administration to rats. *Drug Metabolism and Disposition* **1982,** *10*, 40-46.
46. Jackson, A. J., Intramuscular absorption and regional lymphatic uptake of liposome-entrapped inulin. *Drug Metabolism and Disposition* **1981,** *9*, 535-540.
47. McLennan, D. N.; Porter, C. J. H.; Charman, S. A., Subcutaneous drug delivery and the role of the lymphatics. *Drug Discovery Today: Technologies* **2005,** *2*, 89-96.
48. Oussoren, C.; Zuidema, J.; Crommelin, D.; Storm, G., Lymphatic uptake and biodistribution of liposomes after subcutaneous injection.: II. Influence of liposomal size, lipid composition and lipid dose. *Biochimica et Biophysica Acta (BBA)-Biomembranes* **1997,** *1328*, 261-272.
49. Oussoren, C.; Storm, G., Lymphatic uptake and biodistribution of liposomes after subcutaneous injection: III. Influence of surface modification with poly (ethyleneglycol). *Pharm Res* **1997,** *14*, 1479-1484.
50. Kim, C. K.; Han, J. H., Lymphatic delivery and pharmacokinetics of methotrexate after intramuscular injection of differently charged liposome-entrapped methotrexate to rats. *Journal of microencapsulation* **1995,** *12*, 437-446.

51. Weiss, J.; Decker, E.; McClements, D. J.; Kristbergsson, K.; Helgason, T.; Awad, T., Solid Lipid Nanoparticles as Delivery Systems for Bioactive Food Components. *Food Biophysics* **2008,** *3*, 146-154.
52. Müller, R. H.; Mäder, K.; Gohla, S., Solid lipid nanoparticles (SLN) for controlled drug delivery – a review of the state of the art. *European Journal of Pharmaceutics and Biopharmaceutics* **2000,** *50*, 161-177.
53. Mehnert, W.; Mäder, K., Solid lipid nanoparticles: Production, characterization and applications. *Advanced Drug Delivery Reviews* **2001,** *47*, 165-196.
54. Hu, L.; Tang, X.; Cui, F., Solid lipid nanoparticles (SLNs) to improve oral bioavailability of poorly soluble drugs. *Journal of Pharmacy and Pharmacology* **2004,** *56*, 1527-1535.
55. zur Mühlen, A.; Schwarz, C.; Mehnert, W., Solid lipid nanoparticles (SLN) for controlled drug delivery – Drug release and release mechanism. *European Journal of Pharmaceutics and Biopharmaceutics* **1998,** *45*, 149-155.
56. Jenning, V.; Schäfer-Korting, M.; Gohla, S., Vitamin A-loaded solid lipid nanoparticles for topical use: drug release properties. *Journal of Controlled Release* **2000,** *66*, 115-126.
57. Li, H.; Zhao, X.; Ma, Y.; Zhai, G.; Li, L.; Lou, H., Enhancement of gastrointestinal absorption of quercetin by solid lipid nanoparticles. *Journal of Controlled Release* **2009,** *133*, 238-244.
58. Hussain, N.; Jaitley, V.; Florence, A. T., Recent advances in the understanding of uptake of microparticulates across the gastrointestinal lymphatics. *Advanced Drug Delivery Reviews* **2001,** *50*, 107-142.
59. Khan, A. A.; Mudassir, J.; Mohtar, N.; Darwis, Y., Advanced drug delivery to the lymphatic system: lipid-based nanoformulations. *International Journal of Nanomedicine* **2013,** *8*, 2733-2744.
60. Paliwal, R.; Rai, S.; Vaidya, B.; Khatri, K.; Goyal, A. K.; Mishra, N.; Mehta, A.; Vyas, S. P., Effect of lipid core material on characteristics of solid lipid nanoparticles designed for oral lymphatic delivery. *Nanomedicine: Nanotechnology, Biology and Medicine* **2009,** *5*, 184-191.
61. Bargoni, A.; Cavalli, R.; Caputo, O.; Fundarò, A.; Gasco, M. R.; Zara, G. P., Solid lipid nanoparticles in lymph and plasma after duodenal administration to rats. *Pharm Res* **1998,** *15*, 745-750.
62. Aji Alex, M. R.; Chacko, A. J.; Jose, S.; Souto, E. B., Lopinavir loaded solid lipid nanoparticles (SLN) for intestinal lymphatic targeting. *European Journal of Pharmaceutical Sciences* **2011,** *42*, 11-18.
63. Edwards, G. A.; Porter, C. J. H.; Caliph, S. M.; Khoo, S.-M.; Charman, W. N., Animal models for the study of intestinal lymphatic drug transport. *Advanced Drug Delivery Reviews* **2001,** *50*, 45-60.
64. Porter, C. J.; Charman, S. A.; Charman, W. N., Lymphatic transport of halofantrine in the triple‐cannulated anesthetized rat model: Effect of lipid vehicle dispersion. *Journal of pharmaceutical sciences* **1996,** *85*, 351-356.
65. Porter, C. J.; Charman, S. A.; Humberstone, A. J.; Charman, W. N., Lymphatic transport of halofantrine in the conscious rat when administered as either the free

base or the hydrochloride salt: effect of lipid class and lipid vehicle dispersion. *Journal of pharmaceutical sciences* **1996,** *85*, 357-361.
66. Khoo, S. M.; Edwards, G. A.; Porter, C. J.; Charman, W. N., A conscious dog model for assessing the absorption, enterocyte‐based metabolism, and intestinal lymphatic transport of halofantrine. *Journal of pharmaceutical sciences* **2001,** *90*, 1599-1607.
67. Khoo, S.-M.; Shackleford, D. M.; Porter, C. J.; Edwards, G. A.; Charman, W. N., Intestinal lymphatic transport of halofantrine occurs after oral administration of a unit-dose lipid-based formulation to fasted dogs. *Pharm Res* **2003,** *20*, 1460-1465.
68. Lespine, A.; Chanoit, G.; Bousquet-Melou, A.; Lallemand, E.; Bassissi, F. M.; Alvinerie, M.; Toutain, P.-L., Contribution of lymphatic transport to the systemic exposure of orally administered moxidectin in conscious lymph duct-cannulated dogs. *European journal of pharmaceutical sciences* **2006,** *27*, 37-43.
69. White, D. G.; Story, M. J.; Barnwell, S. G., An experimental animal model for studying the effects of a novel lymphatic drug delivery system for propranolol. *International journal of pharmaceutics* **1991,** *69*, 169-174.
70. Onizuka, M.; FlatebØ, T.; Nicolaysen, G., Lymph flow pattern in the intact thoracic duct in sheep. *The Journal of physiology* **1997,** *503*, 223-234.
71. Segrave, A. M.; Mager, D. E.; Charman, S. A.; Edwards, G. A.; Porter, C. J., Pharmacokinetics of recombinant human leukemia inhibitory factor in sheep. *Journal of Pharmacology and Experimental Therapeutics* **2004,** *309*, 1085-1092.
72. Bocci, V.; Muscettola, M.; Grasso, G.; Magyar, Z.; Naldini, A.; Szabo, G., The lymphatic route. 1) Albumin and hyaluronidase modify the normal distribution of interferon in lymph and plasma. *Experientia* **1986,** *42*, 432-433.
73. Kagan, L.; Gershkovich, P.; Mendelman, A.; Amsili, S.; Ezov, N.; Hoffman, A., The role of the lymphatic system in subcutaneous absorption of macromolecules in the rat model. *European Journal of Pharmaceutics and Biopharmaceutics* **2007,** *67*, 759-765.
74. Dahan, A.; Hoffman, A., Evaluation of a chylomicron flow blocking approach to investigate the intestinal lymphatic transport of lipophilic drugs. *European Journal of Pharmaceutical Sciences* **2005,** *24*, 381-388.
75. Van Greevenbroek, M.; Voorhout, W. F.; Erkelens, D. W.; Van Meer, G.; De Bruin, T., Palmitic acid and linoleic acid metabolism in Caco-2 cells: different triglyceride synthesis and lipoprotein secretion. *Journal of lipid research* **1995,** *36*, 13-24.
76. van Greevenbroek, M. M.; van Meer, G.; Erkelens, D. W.; de Bruin, T. W., Effects of saturated, mono-, and polyunsaturated fatty acids on the secretion of apo B containing lipoproteins by Caco-2 cells. *Atherosclerosis* **1996,** *121*, 139-150.
77. Van Greevenbroek, M.; Robertus-Teunissen, M. G.; Erkelens, D. W.; de Bruin, T., Lipoprotein secretion by intestinal Caco-2 cells is affected differently by trans and cis unsaturated fatty acids: effect of carbon chain length and position of the double bond. *The American journal of clinical nutrition* **1998,** *68*, 561-567.
78. Van Greevenbroek, M.; Erkelens, D.; De Bruin, T., Caco-2 cells secrete two independent classes of lipoproteins with distinct density: effect of the ratio of unsaturated to saturated fatty acid. *Atherosclerosis* **2000,** *149*, 25-31.

79. Caliph, S. M.; Charman, W. N.; Porter, C. J. H., Effect of short-, medium-, and long-chain fatty acid-based vehicles on the absolute oral bioavailability and intestinal lymphatic transport of halofantrine and assessment of mass balance in lymph-cannulated and non-cannulated rats. *Journal of Pharmaceutical Sciences* **2000,** *89*, 1073-1084.
80. Porter, C. J. H.; Charman, W. N., Uptake of drugs into the intestinal lymphatics after oral administration. *Advanced Drug Delivery Reviews* **1997,** *25*, 71-89.
81. Machlin, L. J., *Vitamin E. A comprehensive treatise*. Marcel Dekker, Inc.: 1980.
82. Rucker, R. B.; Suttie, J. W.; McCormick, D. B., *Handbook of vitamins*. CRC Press: 2001.
83. Brigelius-Flohe, R.; Traber, M. G., Vitamin E: function and metabolism. *The FASEB Journal* **1999,** *13*, 1145-1155.
84. RICCIARELLI, R.; ZINGG, J.-M.; AZZI, A., Vitamin E: protective role of a Janus molecule. *The FASEB Journal* **2001,** *15*, 2314-2325.
85. Ju, J.; Picinich, S. C.; Yang, Z.; Zhao, Y.; Suh, N.; Kong, A.-N.; Yang, C. S., Cancer-preventive activities of tocopherols and tocotrienols. *Carcinogenesis* **2010,** *31*, 533-542.
86. Knekt, P.; Aromaa, A.; Maatela, J.; Aaran, R. K.; Nikkari, T.; Hakama, M.; Hakulinen, T.; Peto, R.; Teppo, L., Vitamin E and cancer prevention. *The American Journal of Clinical Nutrition* **1991,** *53*, 283S-286S.
87. Greenwald, P.; Clifford, C. K.; Milner, J. A., Diet and cancer prevention. *European Journal of Cancer* **2001,** *37*, 948-965.
88. Taylor, P. R.; Qiao, Y.-L.; Abnet, C. C.; Dawsey, S. M.; Yang, C. S.; Gunter, E. W.; Wang, W.; Blot, W. J.; Dong, Z.-W.; Mark, S. D., Prospective Study of Serum Vitamin E Levels and Esophageal and Gastric Cancers. *Journal of the National Cancer Institute* **2003,** *95*, 1414-1416.
89. Heinonen, O. P.; Albanes, D., The effect of vitamin E and beta carotene on the incidence of lung cancer and other cancers in male smokers. *The New England journal of medicine (USA)* **1994**.
90. Lee, I.; Cook, N. R.; Gaziano, J.; et al., Vitamin e in the primary prevention of cardiovascular disease and cancer: The women's health study: a randomized controlled trial. *JAMA* **2005,** *294*, 56-65.
91. Lippman, S. M.; Klein, E. A.; Goodman, P. J.; et al., Effect of selenium and vitamin e on risk of prostate cancer and other cancers: The selenium and vitamin e cancer prevention trial (select). *JAMA* **2009,** *301*, 39-51.
92. Jiang, Q.; Christen, S.; Shigenaga, M. K.; Ames, B. N., γ-Tocopherol, the major form of vitamin E in the US diet, deserves more attention. *The American Journal of Clinical Nutrition* **2001,** *74*, 714-722.
93. Li, G.-X.; Lee, M.-J.; Liu, A. B.; Yang, Z.; Lin, Y.; Shih, W. J.; Yang, C. S., δ-Tocopherol Is More Active than α- or γ-Tocopherol in Inhibiting Lung Tumorigenesis In Vivo. *Cancer Prevention Research* **2011,** *4*, 404-413.
94. Guan, F.; Li, G.; Liu, A. B.; Lee, M.-J.; Yang, Z.; Chen, Y.-K.; Lin, Y.; Shih, W.; Yang, C. S., δ- and γ-Tocopherols, but not α-Tocopherol, Inhibit Colon Carcinogenesis in Azoxymethane-Treated F344 Rats. *Cancer Prevention Research* **2012,** *5*, 644-654.

95. Qian, J.; Morley, S.; Wilson, K.; Nava, P.; Atkinson, J.; Manor, D., Intracellular trafficking of vitamin E in hepatocytes: the role of tocopherol transfer protein. *Journal of Lipid Research* **2005,** *46*, 2072-2082.
96. Morley, S.; Cecchini, M.; Zhang, W.; Virgulti, A.; Noy, N.; Atkinson, J.; Manor, D., Mechanisms of Ligand Transfer by the Hepatic Tocopherol Transfer Protein. *Journal of Biological Chemistry* **2008,** *283*, 17797-17804.
97. Li, S.; Pan, M.-H.; Lo, C.-Y.; Tan, D.; Wang, Y.; Shahidi, F.; Ho, C.-T., Chemistry and health effects of polymethoxyflavones and hydroxylated polymethoxyflavones. *Journal of Functional Foods* **2009,** *1*, 2-12.
98. Li, S.; Pan, M.-H.; Lai, C.-S.; Lo, C.-Y.; Dushenkov, S.; Ho, C.-T., Isolation and syntheses of polymethoxyflavones and hydroxylated polymethoxyflavones as inhibitors of HL-60 cell lines. *Bioorganic & Medicinal Chemistry* **2007,** *15*, 3381-3389.
99. Murakami, A.; Nakamura, Y.; Ohto, Y.; Yano, M.; Koshiba, T.; Koshimizu, K.; Tokuda, H.; Nishino, H.; Ohigashi, H., Suppressive effects of citrus fruits on free radical generation and nobiletin, an anti-inflammatory polymethoxyflavonoid. *BioFactors* **2000,** *12*, 187-192.
100. Lai, C.-S.; Li, S.; Chai, C.-Y.; Lo, C.-Y.; Ho, C.-T.; Wang, Y.-J.; Pan, M.-H., Inhibitory effect of citrus 5-hydroxy-3,6,7,8,3′ ,4′ -hexamethoxyflavone on 12-O-tetradecanoylphorbol 13-acetate-induced skin inflammation and tumor promotion in mice. *Carcinogenesis* **2007,** *28*, 2581-2588.
101. Murakami, A.; Nakamura, Y.; Torikai, K.; Tanaka, T.; Koshiba, T.; Koshimizu, K.; Kuwahara, S.; Takahashi, Y.; Ogawa, K.; Yano, M.; Tokuda, H.; Nishino, H.; Mimaki, Y.; Sashida, Y.; Kitanaka, S.; Ohigashi, H., Inhibitory Effect of Citrus Nobiletin on Phorbol Ester-induced Skin Inflammation, Oxidative Stress, and Tumor Promotion in Mice. *Cancer Research* **2000,** *60*, 5059-5066.
102. Tang, M.; Ogawa, K.; Asamoto, M.; Hokaiwado, N.; Seeni, A.; Suzuki, S.; Takahashi, S.; Tanaka, T.; Ichikawa, K.; Shirai, T., Protective effects of citrus nobiletin and auraptene in transgenic rats developing adenocarcinoma of the prostate (TRAP) and human prostate carcinoma cells. *Cancer Science* **2007,** *98*, 471-477.
103. Kurowska, E. M.; Manthey, J. A., Hypolipidemic Effects and Absorption of Citrus Polymethoxylated Flavones in Hamsters with Diet-Induced Hypercholesterolemia. *Journal of Agricultural and Food Chemistry* **2004,** *52*, 2879-2886.
104. Saito, T.; Abe, D.; Sekiya, K., Nobiletin enhances differentiation and lipolysis of 3T3-L1 adipocytes. *Biochemical and Biophysical Research Communications* **2007,** *357*, 371-376.
105. Onda, K.; Horike, N.; Suzuki, T.-i.; Hirano, T., Polymethoxyflavonoids Tangeretin and Nobiletin Increase Glucose Uptake in Murine Adipocytes. *Phytotherapy Research* **2013,** *27*, 312-316.
106. Miyata, Y.; Tanaka, H.; Shimada, A.; Sato, T.; Ito, A.; Yamanouchi, T.; Kosano, H., Regulation of adipocytokine secretion and adipocyte hypertrophy by polymethoxyflavonoids, nobiletin and tangeretin. *Life Sciences* **2011,** *88*, 613-618.

107. Li, S.; Lo, C.-Y.; Ho, C.-T., Hydroxylated Polymethoxyflavones and Methylated Flavonoids in Sweet Orange (Citrus sinensis) Peel. *Journal of Agricultural and Food Chemistry* **2006,** *54*, 4176-4185.
108. Li, S.; Wang, H.; Guo, L.; Zhao, H.; Ho, C.-T., Chemistry and bioactivity of nobiletin and its metabolites. *Journal of Functional Foods* **2014,** *6*, 2-10.
109. Matsuzaki, K.; Yamakuni, T.; Hashimoto, M.; Haque, A. M.; Shido, O.; Mimaki, Y.; Sashida, Y.; Ohizumi, Y., Nobiletin restoring β-amyloid-impaired CREB phosphorylation rescues memory deterioration in Alzheimer's disease model rats. *Neuroscience Letters* **2006,** *400*, 230-234.
110. Nakajima, A.; Yamakuni, T.; Haraguchi, M.; Omae, N.; Song, S.-Y.; Kato, C.; Nakagawasai, O.; Tadano, T.; Yokosuka, A.; Mimaki, Y.; Sashida, Y.; Ohizumi, Y., Nobiletin, a Citrus Flavonoid That Improves Memory Impairment, Rescues Bulbectomy-Induced Cholinergic Neurodegeneration in Mice. *Journal of Pharmacological Sciences* **2007,** *105*, 122-126.
111. Onozuka, H.; Nakajima, A.; Matsuzaki, K.; Shin, R.-W.; Ogino, K.; Saigusa, D.; Tetsu, N.; Yokosuka, A.; Sashida, Y.; Mimaki, Y.; Yamakuni, T.; Ohizumi, Y., Nobiletin, a Citrus Flavonoid, Improves Memory Impairment and Aβ Pathology in a Transgenic Mouse Model of Alzheimer's Disease. *Journal of Pharmacology and Experimental Therapeutics* **2008,** *326*, 739-744.
112. Onoue, S.; Uchida, A.; Takahashi, H.; Seto, Y.; Kawabata, Y.; Ogawa, K.; Yuminoki, K.; Hashimoto, N.; Yamada, S., Development of high-energy amorphous solid dispersion of nanosized nobiletin, a citrus polymethoxylated flavone, with improved oral bioavailability. *Journal of Pharmaceutical Sciences* **2011,** *100*, 3793-3801.
113. Ting, Y.; Li, C. C.; Wang, Y.; Ho, C.-T.; Huang, Q., Influence of Processing Parameters on Morphology of Polymethoxyflavone in Emulsions. *Journal of Agricultural and Food Chemistry* **2015,** *63*, 652-659.
114. Liang, R.; Shoemaker, C. F.; Yang, X.; Zhong, F.; Huang, Q., Stability and Bioaccessibility of β-Carotene in Nanoemulsions Stabilized by Modified Starches. *Journal of Agricultural and Food Chemistry* **2013,** *61*, 1249-1257.
115. Yang, C. S.; Lee, M. J., Methodology of plasma retinol, tocopherol, and carotenoid assays in cancer prevention studies. *J. Nutr., Growth Cancer* **1987,** *4*, 19-27.
116. Zhao, Y.; Lee, M.-J.; Cheung, C.; Ju, J.-H.; Chen, Y.-K.; Liu, B.; Hu, L.-Q.; Yang, C. S., Analysis of Multiple Metabolites of Tocopherols and Tocotrienols in Mice and Humans. *Journal of Agricultural and Food Chemistry* **2010,** *58*, 4844-4852.
117. Yang, X.; Tian, H.; Ho, C.-T.; Huang, Q., Stability of Citral in Emulsions Coated with Cationic Biopolymer Layers. *Journal of Agricultural and Food Chemistry* **2011,** *60*, 402-409.
118. Kaminskas, L. M.; Porter, C. J. H., Targeting the lymphatics using dendritic polymers (dendrimers). *Advanced Drug Delivery Reviews* **2011,** *63*, 890-900.
119. Takakura, Y.; Kitajima, M.; Matsumoto, S.; Hashida, M.; Sezaki, H., Development of a novel polymeric prodrug of mitomycin C, mitomycin C-dextran conjugate with anionic charge. I. Physicochemical characteristics and in vivo and in vitro antitumor activities. *International journal of pharmaceutics* **1987,** *37*, 135-143.

120. Müller, R. H.; Runge, S.; Ravelli, V.; Mehnert, W.; Thünemann, A. F.; Souto, E. B., Oral bioavailability of cyclosporine: Solid lipid nanoparticles (SLN®) versus drug nanocrystals. *International Journal of Pharmaceutics* **2006,** *317*, 82-89.
121. Zara, G. P.; Bargoni, A.; Cavalli, R.; Fundarò, A.; Vighetto, D.; Gasco, M. R., Pharmacokinetics and tissue distribution of idarubicin-loaded solid lipid nanoparticles after duodenal administration to rats. *Journal of Pharmaceutical Sciences* **2002,** *91*, 1324-1333.
122. Li, Y.; Zheng, J.; Xiao, H.; McClements, D. J., Nanoemulsion-based delivery systems for poorly water-soluble bioactive compounds: Influence of formulation parameters on polymethoxyflavone crystallization. *Food Hydrocolloids* **2012,** *27*, 517-528.
123. Ting, Y.; Xia, Q.; Li, S.; Ho, C.-T.; Huang, Q., Design of high-loading and high-stability viscoelastic emulsions for polymethoxyflavones. *Food Research International* **2013,** *54*, 633-640.
124. Hubatsch, I.; Ragnarsson, E. G. E.; Artursson, P., Determination of drug permeability and prediction of drug absorption in Caco-2 monolayers. *Nat. Protocols* **2007,** *2*, 2111-2119.
125. Wang, Z.; Li, S.; Ferguson, S.; Goodnow, R.; Ho, C.-T., Validated reversed phase LC method for quantitative analysis of polymethoxyflavones in citrus peel extracts. *Journal of Separation Science* **2008,** *31*, 30-37.
126. Gelderblom, H.; Verweij, J.; Nooter, K.; Sparreboom, A., Cremophor EL: the drawbacks and advantages of vehicle selection for drug formulation. *European Journal of Cancer* **2001,** *37*, 1590-1598.
127. Hidalgo, I. J.; Raub, T. J.; Borchardt, R. T., Characterization of the human colon carcinoma cell line (Caco-2) as a model system for intestinal epithelial permeability. *Gastroenterology* **1989**, 736-49.
128. Artursson, P.; Palm, K.; Luthman, K., Caco-2 monolayers in experimental and theoretical predictions of drug transport. *Advanced Drug Delivery Reviews* **2012,** *64, Supplement*, 280-289.
129. Artursson, P.; Karlsson, J., Correlation between oral drug absorption in humans and apparent drug permeability coefficients in human intestinal epithelial (Caco-2) cells. *Biochemical and Biophysical Research Communications* **1991,** *175*, 880-885.
130. Yu, H.; Huang, Q., Investigation of the Absorption Mechanism of Solubilized Curcumin Using Caco-2 Cell Monolayers. *Journal of Agricultural and Food Chemistry* **2011,** *59*, 9120-9126.